Article

Alcohol and Water Free Synthesis of Mesoporous Silica Using Deep Eutectic Solvent as a Template and Solvent and Its Application as a Catalyst Support for Formic Acid Dehydrogenation

Dong-Wook Lee, Min-Ho Jin, Ju-Hyoung Park, Young-Joo Lee, Young-Chan Choi, Ji Chan Park, and Dong Hyun Chun

ACS Sustainable Chem. Eng., **Just Accepted Manuscript** • DOI: 10.1021/acssuschemeng.8b02606 • Publication Date (Web): 08 Aug 2018

Alcohol and Water Free Synthesis of Mesoporous Silica Using Deep Eutectic Solvent as a Template and Solvent and Its Application as a Catalyst Support for Formic Acid Dehydrogenation

Dong-Wook Lee,*,† Min-Ho Jin,† Ju-Hyoung Park,‡ Young-Joo Lee,‡ Young-Chan Choi,‡ Ji Chan Park,‡ Dong Hyun Chun‡

† *Advanced Materials and Devices Laboratory, Korea Institute of Energy Research (KIER), 152 Gajeongro, Yuseong, Daejeon 305-343, Republic of Korea*

‡ *Clean Fuel Laboratory, Korea Institute of Energy Research (KIER), 152 Gajeongro, Yuseong, Daejeon 305-343, Republic of Korea*

* *Corresponding Author E-mail: dwlee99@kier.re.kr*

Abstract

Synthetic methods of mesoporous silica using surfactants or ionic liquids as a template have several disadvantages to commercialization such as low economic feasibility and low sustainability. Thus, the development of more ecofriendly and economical synthetic pathways for commercialization of mesoporous silica remains a challenge in the field of mesoporous silica synthesis. In this study, we first report a synthetic method of mesoporous silica (KIE-11) using deep eutectic solvent (DES) of choline chloride/urea as a templating agent and solvent without alcohol and water, except for water needed for hydrolysis of tetraethyl orthosilicate. KIE-11 has very high surface area (up to 877 m^2/g) and pore volume (up to 1.74 cm^3/g), and its pore size can be easily tailored from 3.3 nm up to 24.5 nm with narrow pore size distribution by only changing the aging conditions. On the basis of various analyses of KIE-11, we deduced pore formation mechanism of mesoporous silica by DES. In addition, we used KIE-11 as a catalyst support for additive-free formic acid dehydrogenation at room-temperature, and KIE-11-supported catalysts showed excellent catalytic activity (TOF: 860.7 mol H_2 mol Pd^{-1} h^{-1}). Comparing to surfactant or ionic liquid-templated methods, the DES-templated synthetic method is much cheaper, more ecofriendly, and more energy efficient. Therefore this work is expected to open a new avenue for cheap and green synthesis of mesoporous silica on an industrial scale.

KEYWORDS: *Deep eutectic solvent, Mesoporous silica, Choline Chloride, Urea, Formic acid dehydrogenation*

INTRODUCTION

Since MCM-41 was first synthesized in 1992,[1,2] there has been intense research activity in preparation of mesoporous silica materials with various pore structure using ionic[3-5] and neutral[6-9] surfactants as a templating agent. However, in spite of their well-defined pore structure, synthetic methods of mesoporous silica using surfactant templates have main two disadvantages to commercialization. First, ionic and neutral surfactants are expensive and have low biodegradability originating from their long hydrophobic organic segments. Second, the synthetic methods usually require excess solvent such as water or alcohol, which leads to a decrease in economic feasibility because of unnecessary energy consumption to heat up the excess solvent during synthesis and the necessity of removal or recovery processes of solvent. In addition, when hydrothermal treatment is used to tailor pore size without changing surfactants, high pressure reactors are needed because of high vapor pressure of excess solvent. For such reasons, recently, ionic liquids as a templating agent for synthesis of mesoporous silica were used to improve the sustainability and economic feasibility of the synthetic method,[10-19] as ionic liquids have unique properties such as low vapor pressure, high thermal and chemical stability, and high ionic conductivity. However, ionic liquids are also very expensive and not ecofriendly as are surfactant templates. In addition, excess water and alcohol are still needed to synthesize mesoporous silica. These disadvantages interrupt the applications of ionic liquid-templated mesoporous silica on an industrial scale. Thus, the development of more ecofriendly and economical synthetic pathways for commercialization of mesoporous silica remains a challenge in the field of mesoporous silica synthesis.[20,21]

In this study, we first report a synthetic method of mesoporous silica (KIE-11) using deep eutectic solvent (DES) of choline chloride/urea as a templating agent and solvent without alcohol and water, except for water needed for hydrolysis of tetraethyl orthosilicate (TEOS). We found that pore size can be easily tailored up to 24.5 nm with high surface area and pore volume by only changing the aging conditions. DES has similarities with ionic liquids such as low vapor pressure, high thermal and chemical stability, and DES is stable in air, much cheaper, and greener than ionic liquids.[22-25] Moreover, in our study, DES did not need other solvents during synthesis of mesoporous silica. Thus, when thermal treatment in a sealed reactor at elevated temperature was conducted to tailor pore size larger, the internal pressure

of the sealed reactor was lower than that under thermal treatment condition using excess water and alcohol. Therefore the DES-templated synthetic method has much higher sustainability and economic feasibility in comparison with surfactant and ionic liquid-templated methods. To the best of our knowledge, this work is the first report on the preparation of mesoporous silica using DES as a template and solvent,[26] and is expected to open a new avenue for cheap and green synthesis of mesoporous silica.

EXPERIMENTAL SECTION

Preparation of DES and Silica Sol. DES as a templating agent and solvent for synthesis of mesoporous silica KIE-11 was prepared by mixing of choline chloride and urea and thermal treatment of the mixture at 90 ^{o}C.[22] The molar ratio of choline chloride and urea was 1:2, and addition amount of choline chloride and urea for each KIE-11 sample is shown in Table 1. In addition, silica sol as a nano building block for silica framework of KIE-11 was prepared by hydrolysis and condensation of tetraethyl orthosilicate (TEOS: 98%, Aldrich) at room temperature under acid catalyzed condition. In a typical synthesis, 13.4 mL of TEOS, 6.2 mL of distilled water, and 0.36 mL of nitric acid were mixed and vigorously stirred at room temperature for 20 min, resulting in transparent silica sol.

Preparation of Mesoporous Silica without Aging. 13 g of the as-prepared DES and 20 mL of silica sol were mixed and vigorously stirred (0 g of DES for KIE-11-a, 6.5 g of DES for KIE-11-b, 26 g of DES for KIE-11-d, 52 g of DES for KIE-11-e). After the mixture of DES and silica sol was calcined in a muffle furnace at 600 ^{o}C for 3 h, mesoporous silica KIE-11 was prepared.

Preparation of Mesoporous Silica by Aging in a Muffle Furnace. 13 g of the as-prepared DES and 20 mL of silica sol were mixed and vigorously stirred. The mixture of DES and silica sol was thermally aged in a muffle furnace at 60 ^{o}C - 180 ^{o}C for 24 h, followed by calcination in a muffle furnace at 600 ^{o}C for 3 h, resulting in mesoporous silica KIE-11.

Preparation of Ultra-Large-Pore Mesoporous Silica by Aging in an Autoclave. 13 g of the as-prepared DES and 20 mL of silica sol were mixed and vigorously stirred. The mixture of DES and silica sol was thermally aged in a Teflon-lined autoclave at 100 ^{o}C - 180 ^{o}C for 24 h under autogenous pressure (internal pressure less than 4 bar was detected because of a little amount of water added for hydrolysis of TEOS and ethanol formed by condensation), and after cooling the samples to room temperature, the samples were transferred to a muffle furnace. After calcination in a muffle furnace at 600 ^{o}C for 3 h, ultra-large-pore KIE-11 was successfully obtained.

Characterization. The pore properties of mesoporous silica materials were taken by nitrogen sorption tests with a Micromeritics ASAP 2420 instrument. Degassing of samples

was conducted at 200 ^{o}C for 5 h. Transmission electron microscopy (TEM) and scanning transmission electron microscopy (STEM) analyses were conducted by using a FEI/TECNAI G2 instrument. Thermal gravimetric analysis (TGA) was conducted at a heating rate of 20 ^{o}C/min and a nitrogen flow rate of 100 mL/min on a Q500 TA instrument. Inductively coupled plasma atomic emission spectroscopy (ICP-AES) analyses were conducted using Thermo Scientific iCAP 6500.

Preparation of KIE-11-Supported Catalysts for Additive-Free Dehydrogenation of Formic Acid at Room Temperature. As a formic acid dehydrogenation catalyst, we prepared Pd/NH_2-KIE-11 using KIE-11-c, KIE-11-h, KIE-11-j, KIE-11-k, and KIE-11-l as a catalyst support. In a typical synthesis, 0.1 g of KIE-11-c (KIE-11-h, KIE-11-j, KIE-11-k or KIE-11-l) was added into 30 mL of toluene, followed by addition of 0.25 mL of 3-aminopropyl trimethoxysilane (APTMS: Aldrich, 97%). The final mixture was refluxed without stirring for 3 h at 110 ^{o}C. After filtering and washing unreacted APTMS with toluene, NH_2-functionalized KIE-11 samples were successfully prepared. Subsequently, 25.3 mg of palladium(II) nitrate hydrate (Aldrich 205761) was added into 10 mL of distilled water, and then 0.18 g of NH_2-KIE-11-c (NH_2-KIE-11-h, NH_2-KIE-11-j, NH_2-KIE-11-k or NH_2-KIE-11-l) was added into the solution, followed by vigorous stirring for 6 h. Afterward, 2 mL of 0.85 M $NaBH_4$ aqueous solution was added into the mixture solution, followed by stirring for 1 h. After centrifugation, washing, and drying, the Pd/NH_2-KIE-11 catalysts were successfully prepared.

Additive-Free Dehydrogenation of Formic Acid at Room Temperature. 0.055g of Pd-/NH_2-KIE-11 was sealed in a 100mL Teflon-lined reactor, followed by a nitrogen purge for 30 min. After the nitrogen purge, the outlet of the reactor was connected to a gas burette system filled with water. Subsequently, a mixture of 10 mL of distilled water and 0.19 mL of formic acid (95%, Aldrich) was injected into the reactor through a rubber septum. The volume of gas generated at 25 ^{o}C without stirring was measured by the gas burette system. A turnover frequency (TOF) was calculated from the equation as follows.

$$TOF = PV/(2RTn_{Pd}t) \quad (1)$$

Where P is the atmospheric pressure (101325 Pa), V is the produced H_2/CO_2 gas volume when conversion reaches 20 %, R is the universal gas constant (8.3145 m^3 Pa mol^{-1} K^{-1}), T is

298 K, n_{Pd} is the mole number of Pd in Pd/NH_2-KIE-11 catalysts, and t is the reaction time when 20 % of conversion was achieved.[30,31]

RESULTS AND DISCUSSION

DES as a Pore Forming Agent and Solvent for Synthesis of Mesoporous Silica. We used DES of choline chloride/urea to synthesize mesoporous silica, and investigated whether DES of choline chloride and urea plays a significant role as a pore forming agent and solvent simultaneously. During the synthesis of mesoporous silica, other solvent and pore forming agents were not used except for a little amount of water required for hydrolysis of TEOS. In addition, we also observed the effect of content of DES on pore properties such as surface area, pore volume, and pore size. Figure 1 shows nitrogen sorption isotherms and pore size distributions of KIE-11-a, KIE-11-b, KIE-11-c, KIE-11-d and KIE-11-e. In the case of KIE-11-a prepared by drying and calcination of silica sol without addition of DES, it gave a typical type I isotherm with no hysteresis loops and pore diameter was below 2 nm, which demonstrates that KIE-11-a has microporous structure. However, as for KIE-11-b synthesized by using DES as a pore forming agent and solvent, it showed a type IV isotherm with an obvious H2 hysteresis loop, indicating that mesoporous structure was successfully established by addition of DES, and DES of choline chloride and urea plays a significant role as a pore forming agent and solvent simultaneously. In addition to the increase of pore size to mesopore range, specific surface area and pore volume of KIE-11-b remarkably increased from 201 m^2/g and 0.1 cm^3/g to 786 m^2/g and 0.66 cm^3/g, respectively (Table 2). KIE-11-c, KIE-11-d, and KIE-11-e were also prepared by increasing the content of DES. They also gave type IV isotherms with obvious H2 hysteresis loops and comparing to KIE-11-b, their pore size and pore volume increased from 3.5 nm and 0.66 cm^3/g to 6.6 nm and 0.91 cm^3/g, respectively (Table 2). On the basis of such results, it was also revealed that pore size of mesoporous silica KIE-11 can be tailored by changing the content of DES. Figures 2 and S1 show TEM images of mesoporous silica KIE-11-c. The framework of KIE-11-c consists of interconnected silica nanoparticles with particle size of about 7 nm, and its pore structure is three dimensionally interconnected wormhole mesopore structure. The wormhole mesopores were derived from the interstitial void of silica nanoparticles interconnected by condensation of surface silanol groups.

Pore Size Control of KIE-11 by Aging in a Muffle Furnace. For expansion of pore size of KIE-11 without increasing the content of DES, we introduced an aging process into the

synthetic method. While temperature was raised to 600 ^{o}C, KIE-11 samples were thermally aged in a muffle furnace at arbitrary temperature in the range of 60 ^{o}C – 180 ^{o}C for 24 h. Figure 3 shows nitrogen sorption isotherms and pore size distributions of KIE-11-f (aging at 60 ^{o}C), KIE-11-g (aging at 100 ^{o}C), KIE-11-h (aging at 130 ^{o}C), and KIE-11-i (aging at 180 ^{o}C). All of the samples provided type IV isotherms with H2 hysteresis loops in the relative pressure range of 0.40 – 0.85. Comparing to KIE-11-c synthesized without the aging process, as aging temperature increased from 60 ^{o}C to 130 ^{o}C, pore size and pore volume gradually increased up to 5.8 nm and 1.06 cm^3/g, and specific surface area increased from 707 m^2/g up to 877 m^2/g, followed by a slight decrease to 821 m^2/g (Table 2). However, when aging temperature increased from 130 ^{o}C (KIE-11-h) to 180 ^{o}C (KIE-11-i), pore size and pore volume of KIE-11 dramatically decreased from 5.8 nm and 1.06 cm^3/g to 3.3 nm and 0.48 cm^3/g (Table 2). Figures 4 and S2 present TEM images of KIE-11-g (aging at 100 ^{o}C) and KIE-11-i (aging at 180 ^{o}C). Both of KIE-11-g and KIE-11-i samples have three dimensionally interconnected wormhole mesopore structure, originating from the interstitial void of silica nanoparticles with particle size of about 7 nm. However, comparing to KIE-11-g, pore size of KIE-11-i significantly decreased.

To investigate the reason why the unexpected decrease in pore properties of KIE-11 occurred at 180 ^{o}C of aging temperature, we conducted thermal gravimetric analysis (TGA) for silica sol, DES (choline chloride/urea), and mixture of silica sol and DES (choline chloride/urea). Figure 5 presents TGA curves for silica sol, DES, and mixture of silica sol and DES. In the case of silica sol, there were three weight loss regions below 100 ^{o}C, 100 ^{o}C – 200 ^{o}C, and above 350 ^{o}C. The weight loss below 100 ^{o}C is attributed to evaporation of water added for hydrolysis of TEOS and ethanol formed by condensation. The weight loss in the temperature range between 100 ^{o}C and 200 ^{o}C originates from coalescence of silica nanoparticles through condensation of surface silanol groups. In addition, the weight loss above 350 ^{o}C is derived from elimination of chemically bound water.[27] As for DES of choline chloride and urea, there was a main weight loss region between 170 ^{o}C and 350 ^{o}C (Figures 5 and S3), which is attributed to volatilization or decomposition of DES. When silica sol and DES were mixed, three weight loss regions were observed at below 100 ^{o}C, 100 ^{o}C – 170 ^{o}C, and 170 ^{o}C - 350 ^{o}C (Figures 5 and S3), which is assigned to evaporation of water and ethanol, condensation of surface silanol groups, and decomposition of DES (choline

chloride/urea), respectively. In summary, as shown in Figure 6, while mixture of silica sol and DES is thermally treated, robust framework structure of KIE-11 is formed by coalescence of silica nanoparticles through condensation of surface silanol groups in the temperature range of 100 ^{o}C – 200 ^{o}C, and decomposition of DES as a pore forming agent occurs in the temperature range of 170 ^{o}C – 350 ^{o}C. Interestingly, in the temperature range between 170 ^{o}C and 200 ^{o}C, coalescence of silica nanoparticles occurs simultaneously with decomposition of DES as a pore forming agent. In other words, decomposition of DES before formation of robust silica framework by enough coalescence of silica nanoparticles can incur collapse or shrinkage of silica framework in the temperature range of 170 ^{o}C - 200 ^{o}C. Thus, when expansion of pore size by aging in a muffle furnace is desired, the aging temperature range between 100 ^{o}C and 170 ^{o}C is the most suitable for maintaining expanded pore volume against collapse of framework by decomposition of DES as a pore forming agent. This is because, in only such a temperature range, robust silica framework can be formed with DES included inside silica framework.

Pore Size Control of KIE-11 by Aging in an Autoclave. For further expansion of pore size of KIE-11, we also investigated the variation behavior of pore structure of KIE-11 by aging in an autoclave. Before calcination at 600 ^{o}C, KIE-11 samples were aged in an autoclave at arbitrary temperature in the range of 100 ^{o}C – 180 ^{o}C for 24 h. In spite of heating an autoclave up to 180 ^{o}C, the internal pressure of the autoclave was less than 4 bar, which is lower than that under hydrothermal condition with excess water and alcohol. Figure 7 shows nitrogen sorption isotherms and pore size distributions of KIE-11-j (aging at 100 ^{o}C in an autoclave), KIE-11-k (aging at 130 ^{o}C in an autoclave), and KIE-11-l (aging at 180 ^{o}C in an autoclave). All of the samples gave type IV isotherms with H2 hysteresis loops in the relative pressure range of 0.4 – 1.0. As aging temperature in an autoclave increased, the hysteresis loop significantly shifted toward higher relative pressure, which indicates a dramatic increase in pore size. As shown in Figure 7b and Table 2, as aging temperature increased up to 180 ^{o}C, pore size and pore volume remarkably increased from 3.6 nm and 0.64 cm^3/g up to 24.5 nm and 1.74 cm^3/g, and specific surface area gradually decreased. In the case of aging in a muffle furnace, aging at 180 ^{o}C resulted in a significant decrease in pore size and pore volume because of collapse of silica framework by volatilization or decomposition of DES before formation of robust framework. However, in the case of aging in an autoclave, very large

pore size and very high pore volume were achieved in spite of aging at 180 ^{o}C, and pore size and pore volume significantly increased in comparison with KIE-11-k prepared by aging in an autoclave at 130 ^{o}C.

Comparing KIE-11-g with KIE-11-j, KIE-11-h with KIE-11-k, and KIE-11-i with KIE-11-l, although the aging temperature was the same each other, KIE-11 samples synthesized by aging in an autoclave have much larger pore size and higher pore volume than those synthesized by aging in a muffle furnace (Table 2). To investigate such phenomena, TEM analyses for KIE-11-j, KIE-11-k, and KIE-11-l were conducted. As shown in Figures 8 and S4, the silica nanoparticle size of the framework of KIE-11-j, KIE-11-k, and KIE-11-l was about 8.7 nm, 9.3 nm, and 12 nm, respectively. Comparing to the silica nanoparticle size for KIE-11 prepared by aging in a muffle furnace (Figures 4 and S2), the silica nanoparticle size for KIE-11 synthesized by aging in an autoclave increased (Figures 8 and S4). Such an increase in the silica nanoparticle size by aging in an autoclave could be ascribed to dissolution and recondensation of preformed silica nanoparticles under hydrothermal condition.[28,29] Unlike aging in a muffle furnace, aging in an autoclave created hydrothermal condition because of the presence of water which was added for hydrolysis of TEOS. Thus the increase in silica nanoparticle size under hydrothermal condition in an autoclave gave rise to expansion of interstitial volume among silica nanoparticles and an increase in amount of DES embedded inside silica framework. In addition, thick and robust framework structure of KIE-11 was formed by the dissolution and recondensation of preformed silica nanoparticles under hydrothermal condition. The thick and robust silica framework structure with large silica nanoparticle size suppressed the collapse of silica framework and decrease in pore size even at 180 ^{o}C, where decomposition of DES occurs. This is the reason why pore size and pore volume of KIE-11 synthesized by aging in an autoclave were much higher than those of KIE-11 synthesized by aging in a muffle furnace.

Pore Formation Mechanism of KIE-11. On the basis of results mentioned above, we deduced the pore formation mechanism for mesoporous silica KIE-11 prepared by using DES of choline chloride/urea as a templating agent and solvent. Figure 9 shows pore formation mechanism of KIE-11. Nanocomposites between silica nanoparticles and DES can be easily formed by thermal treatment of mixture solution of silica sol and DES (choline chloride/urea). When the nanocomposite is directly calcined without aging, elimination rate of DES is much

faster than formation rate of robust silica framework through condensation of surface silanol groups. Therefore, expanded pore structure, originating from space occupied by DES, is significantly collapsed, because DES is eliminated from silica framework before formation of robust framework. Likewise, in the case of aging in a muffle furnace above 170 ^{o}C, DES is quickly eliminated from silica framework, resulting in collapse of expanded pore structure and corresponding decrease in pore size. However, when aging in a muffle furnace is conducted in the temperature range of 100 ^{o}C – 170 ^{o}C, robust silica framework can be formed by condensation of surface silanol groups before elimination of DES from the silica framework. Eventually, as the expanded pore structure is kept even after calcination at 600 ^{o}C, large-pore mesoporous silica can be successfully obtained. When the nanocomposite of silica and DES is aged in an autoclave above 100 ^{o}C, we can also synthesize ultra-large-pore mesoporous silica. As hydrothermal condition is created in an autoclave by a little amount of water which is added for hydrolysis of TEOS, dissolution and recondensation of preformed silica nanoparticles occur under the hydrothermal condition. Thus nanoparticle size of silica as a nano building block for framework increases, and thick and robust silica framework can be formed. Such thick and robust silica framework structure is a crucial factor to obtain ultra-large-pore mesoporous silica, because collapse of framework during elimination of DES is easily suppressed.

Additive-Free Dehydrogenation of Formic Acid at Room Temperature. To verify the performance of KIE-11 as a catalyst support, we prepared Pd/NH_2-KIE-11 catalysts for additive-free formic acid dehydrogenation at room-temperature. The Pd loading contents for Pd/NH_2-KIE-11-c, Pd/NH_2-KIE-11-k, and Pd/NH_2-KIE-11-l catalysts were estimated to be 5.8, 5.9, and 5.8 wt% respectively by ICP-AES. Figure 10 shows formic acid dehydrogenation results for Pd/NH_2-KIE-11 catalysts. In the case of the Pd/NH_2-KIE-11-k catalyst, 218 mL of H_2 and CO_2 was produced at 35 min of reaction time, and a turnover frequency (TOF) at 25 ^{o}C and 20 % of conversion was 860.7 mol H_2 mol Pd^{-1} h^{-1} (Table S1), which is excellent catalytic activity compared to previous publications for additive-free formic acid dehydrogenation at room-temperature.[31-34] In addition, the volumetric ratio of H_2 to CO_2 was 50.9:49.1 (Figure S5), and CO was not detected (detection limit < 10 ppm). However, TOFs of Pd/NH_2-KIE-11-c and Pd/NH_2-KIE-11-l catalysts were 257.0 mol H_2 mol Pd^{-1} h^{-1} and 151.0 mol H_2 mol Pd^{-1} h^{-1} (Table S1), which is much lower than that of the

Pd/NH_2-KIE-11-k catalyst. Figure S6 shows a TEM image of Pd/NH_2-KIE-11-k catalysts. After NH_2 functionalization and Pd impregnation, the three dimensionally interconnected wormhole mesopore structure of KIE-11-k shown in Figure 8b was successfully maintained, which indicates that NH_2 groups were successfully functionalized inside the pores of KIE-11. Figure 11 shows STEM images of Pd/NH_2-KIE-11-c, Pd/NH_2-KIE-11-k, and Pd/NH_2-KIE-11-l catalysts. Whereas the average Pd particle size of the Pd/NH_2-KIE-11-c and Pd/NH_2-KIE-11-k catalysts was 1.75 nm and 1.60 nm, that of the Pd/NH_2-KIE-11-l catalysts was 2.58 nm. Moreover, in the case of the Pd/NH_2-KIE-11-l catalysts, parts of Pd nanoparticles were aggregated. As Pd nanoparticle size decreased, the catalytic activity of Pd/NH_2-KIE-11 catalysts increased. In addition, the Pd nanoparticle size is considered to be determined by the pore structure of KIE-11.

Even though those catalysts had the same component and content, they gave very different catalytic activity as the pore structure of catalyst supports and corresponding Pd nanoparticle size were changed. Large mesopores of catalyst supports provide easy diffusion of reactant molecules toward active sites and product molecules away from active sites, while small mesopores with high surface area provide the confinement of active metal nanoparticles to the pores of supports and suppress the aggregation of active metal nanoparticles. Thus KIE-11-k seems to have a tradeoff pore structure between easy diffusion of molecules and confinement of active metal nanoparticles, which results in higher catalytic activity of the Pd/NH_2-KIE-11-k catalyst. In contrast, the pore size of KIE-11-c did not provide the easy diffusion of reactant and product molecules, and large pore size of KIE-11-l did not give the confinement effect of active metal nanoparticles to the pores of supports, which resulted in the increase in Pd nanoparticle size and aggregation of Pd nanoparticles. On the basis of such a result, we demonstrated that the pore structure of KIE-11 support is a very significant factor to determine the catalytic activity for additive-free formic acid dehydrogenation at room-temperature, because diffusion of molecules and Pd nanoparticle size are determined by the pore structure of KIE-11. Thus it was revealed that tailoring pore structure of support materials can be a significant technology to design catalysts with higher catalytic activity.

CONCLUSIONS

We prepared mesoporous silica KIE-11 using DES of choline chloride/urea as a templating agent and solvent without alcohol and water, except for water needed for hydrolysis of TEOS. On the basis of various results for KIE-11, we could draw conclusions as follows.

(1) Mesoporous structure of KIE-11 was successfully established by using DES as a template and solvent. Pore size of KIE-11 can be tailored up to 24.5 nm by changing the content of DES or aging condition, and pore structure of KIE-11 is three dimensionally interconnected wormhole mesopore structure.

(2) We deduced the pore formation mechanism of KIE-11. In the case of synthesis without aging or with aging in a muffle furnace above 170 ^{o}C, elimination rate of DES is much faster than formation rate of robust silica framework. Therefore, expanded pore structure is significantly collapsed. However, in the case of aging in a muffle furnace at 100 ^{o}C – 170 ^{o}C, as robust silica framework is formed before elimination of DES, large-pore mesoporous silica can be successfully obtained. In the case of aging in an autoclave above 100 ^{o}C, as silica nanoparticle size of framework increases under hydrothermal condition, thick and robust silica framework is formed under the hydrothermal condition. Thus collapse of framework during elimination of DES is easily suppressed, resulting in formation of ultra-large-pore mesoporous silica.

(3) KIE-11 was used as a catalyst support for additive-free formic acid dehydrogenation at room-temperature, and KIE-11-supported catalysts showed excellent catalytic activity (TOF: 860.7 mol H_2 mol Pd^{-1} h^{-1}). In addition, it was confirmed that the pore structure of KIE-11 supports is a very significant factor to determine the catalytic activity.

Supporting Information

The Supporting Information is available free of charge on the ACS Publications website at DOI: 10.1021/acssuschemeng.

High magnification TEM images of KIE-11 samples, DTG curves of DES and mixture of silica sol and DES, GC spectrum for the produced gas from formic acid aqueous solution over the Pd/NH_2-KIE-11-k catalyst, TEM image of the Pd/NH_2-KIE-11-k catalyst, and formic acid dehydrogenation activity of Pd/NH_2-KIE-11 catalysts.

Corresponding Author

* E-mail: dwlee99@kier.re.kr

Notes

The authors declare no competing financial interest.

ACKNOWLEDGMENTS

This work was supported by research programs (B7-2461-03, B8-2432-02) of the Korea Institute of Energy Research (KIER).

REFERENCES

(1) Kresge, C.T.; Leonowicz, M.E.; Roth, W.J.; Vartuli, J.C.; Beck, J.S. Ordered Mesoporous Molecular Sieves Synthesized by a Liquid-Crystal Template Mechanism. *Nature* **1992**, *359*, 710-712, DOI 10.1038/359710a0.

(2) Beck, J.S.; Vartuli, J.C.; Roth, W.J.; Leonowicz, M.E.; Kresge, C.T.; Schmitt, K.D.; Chu, C.T-W.; Olson, D.H.; Sheppard, E.W.; McCullen, S.B.; Higgins, J.B.; Schlenker, J.L. A New Family of Mesoporous Molecular Sieves Prepared with Liquid Crystal Templates. *J. Am. Chem. Soc.* **1992**, *114*, 10834-10843, DOI 10.1021/ja00053a020.

(3) Huo, Q.; Margolese, D.I.; Ciesla, U.; Feng, P.; Gier, T.E.; Sieger, P.; Leon, R.; Petroff, P.M.; Schüth, F.; Stucky, G.D. Generalized Synthesis of Periodic Surfactant/Inorganic Composite Materials. *Nature* **1994**, *368*, 317-321, DOI 10.1038/368317a0.

(4) Yang, H.; Kuperman, A.; Coombs, N.; Mamiche-Afara, S.; Ozin, G.A. Synthesis of Oriented Films of Mesoporous Silica on Mica. *Nature* **1996**, *379*, 703-705, DOI 10.1038/379703a0.

(5) Huo, Q.; Margolese, D.I.; Stucky, G.D. Surfactant Control of Phases in the Synthesis of Mesoporous Silica-Based Materials. *Chem. Mater.* **1996**, *8*, 1147-1160, DOI 10.1021/cm960137h.

(6) Tanev, P.T.; Pinnavaia, T.J. A Neutral Templating Route to Mesoporous Molecular Sieves. *Science* **1995**, *267*, 865-867, DOI 10.1126/science.267.5199.865.

(7) Bagshaw, S.A.; Prouzet, E.; Pinnavaia, T.J. Templating of Mesoporous Molecular Sieves by Nonionic Polyethylene Oxide Surfactants. *Science* **1995**, *269*, 1242-1244, DOI 10.1126/science.269.5228.1242.

(8) Attard, G.S.; Glyde, J.C.; Göltner, C.G. Liquid-Crystalline Phases as Templates for the Synthesis of Mesoporous Silica. *Nature* **1995**, *378*, 366-368, DOI 10.1038/378366a0.

(9) Zhao, D.; Huo, Q.; Feng, J.; Chmelka, B.F.; Stucky, G.D. Nonionic Triblock and Star Diblock Copolymer and Oligomeric Surfactant Synthesis of Highly Ordered, Hydrothermally Stable, Mesoporous Silica Structure. *J. Am. Chem. Soc.* **1998**, *120*, 6024-6036, DOI 10.1021/ja974025i.

(10) Dai, S.; Ju, Y.H.; Gao, H.J.; Lin, J.S.; Pennycook, S.J.; Barnes, C.E. Preparation of Silica Aerogel Using Ionic Liquids as Solvents. *Chem. Commun.* **2000**, 243-244, DOI 10.1039/A907147D.

(11) Zhou, Y.; Antonietti, M. Preparation of Highly Ordered Monolithic Super-Microporous Lamellar Silica with a Room-Temperature Ionic Liquid as Template via the Nanocasting Technique. *Adv. Mater.* **2003**, *15*, 1452-1455, DOI 10.1002/adma.200305265.

(12) Trewyn, B.G.; Whitman, C.M.; Lin, V.S.-Y. Morphological Control of Room-Temperature Ionic Liquid Templated Mesoporous Silica Nanoparticles for Controlled Release of Antibacterial Agents. *Nano Lett.* **2004**, *4*, 2139-2143, DOI 10.1021/nl048774r.

(13) Dattelbaum, A.M.; Baker, S.N.; Baker, G.A. *N*-alkyl-*N*-methylpyrrolidinium Salts as Templates for Hexagonally Meso-Ordered Silicate Thin Films. *Chem. Commun.* **2005**, 939-941, DOI 10.1039/b415135f.

(14) Wang, T.; Kaper, H.; Antonietti, M.; Smarsly, B. Templating Behavior of a Long-Chain Ionic Liquid in the Hydrothermal Synthesis of Mesoporous Silica. *Langmuir* **2007**, *23*, 1489-1495, DOI 10.1021/la062470y.

(15) Ma, Z.; Yu, J.; Dai, S. Preparation of Inorganic Materials Using Ionic Liquids. *Adv. Mater.* **2010**, *22*, 261-285, DOI 10.1002/adma.200900603.

(16) Jones, B.H.; Lodge, T.P. Hierarchically Porous Silica Prepared from Ionic Liquid and Polymeric Bicontinuous Microemulsion Templates. *Chem. Mater.* **2011**, *23*, 4824-4831, DOI 10.1021/cm202170g.

(17) Chen, Z.; Greaves, T.L.; Caruso, R.A.; Drummond, C.J. Long-Range Ordered Lyotropic Liquid Crystals in Intermediate-Range Ordered Protic Ionic Liquid Used as Templates for Hierarchically Porous Silica. *J. Mater. Chem.* **2012**, *22*, 10069-10076, DOI 10.1039/C2JM30708A.

(18) Pujari, A.A.; Chadbourne, J.J.; Ward, A.J.; Costanzo, L.; Masters, A.F.; Maschmeyer, T. The Use of Acidic Task-Specific Ionic Liquids in the Formation of High Surface Area Mesoporous Silica. *New J. Chem.* **2009**, *33*, 1997-2000, DOI 10.1039/B907077J.

(19) Du, Z.; Li, E.; Wang, G.; Cheng, F. Thermostable Mesoporous Silica Nanospheres Produced through the Use of a Trisiloxane-Tailed Ionic Liquid as a Template. *RSC Adv.* **2014**, *4*, 4836-4838, DOI 10.1039/C3RA46519E.

(20) Gérardin, C.; Reboul, J.; Bonne, M.; Lebeau, B. Ecodesign of Ordered Mesoporous Silica Materials. *Chem. Soc. Rev.* **2013**, *42*, 4217-4255, DOI 10.1039/C3CS35451B.

(21) Perego, C.; Millini, R. Porous Materials in Catalysis: Challenges for Mesoporous Materials. *Chem. Soc. Rev.* **2013**, *42*, 3956-3976, DOI 10.1039/C2CS35244C.

(22) Abbott, A.P.; Capper, G.; Davies, D.L.; Rasheed, R.K.; Tambyrajah, V. Novel Solvent Properties of Choline Chloride/Urea Mixtures. *Chem. Commun.* **2003**, 70-71, DOI 10.1039/B210714G.

(23) Cooper, E.R.; Andrews, C.D.; Whestley, P.S.; Webb, P.B.; Wormald, P.; Morris, R.E. Ionic Liquids and Eutectic Mixtures as Solvent and Template in Synthesis of Zeolite Analogues. *Nature* **2004**, *430*, 1012-1016, DOI 10.1038/nature02860.

(24) Ranganathan, S.; Zeitlhofer, S.; Sieber, V. Development of a Lipase-Mediated Epoxidation Process for Monoterpenes in Choline Chloride-Based Deep Eutectic Solvents. *Green Chem.* **2017**, *19*, 2576-2586, DOI 10.1039/C7GC01127J.

(25) Abbott, A.P.; Al-Bassam A.Z.M.; Goddard, A.; Harris, R.C.; Jenkin, G.R.T.; Nisbet, F.J.; Wieland, M. Dissolution of Pyrite and Other Fe-S-As Minerals Using Deep Eutectic Solvents. *Green Chem.* **2017**, *19*, 2225-2233, DOI 10.1039/C7GC00334J.

(26) Ge, X.; Gu, C.; Wang, X.; Tu, J. Deep Eutectic Solvents (DESs)-Derived Advanced Functional Materials for Energy and Environmental Applications: Challenges, Opportunities, and Future Vision. *J. Mater. Chem. A* **2017**, *5*, 8209-8229, DOI 10.1039/C7TA01659J.

(27) Mueller, R.; Kammler, H.K.; Wegner, K.; Pratsinis, S.E. OH Surface Density of SiO_2 and TiO_2 by Thermogravimetric Analysis. *Langmuir* **2003**, *19*, 160-165, DOI 10.1021/la025785w.

(28) Galarneau, A.; Iapichella, J.; Bonhomme, K.; Renzo, F.D.; Kooyman, P.; Terasaki, O.; Fajula, F. Controlling the Morphology of Mesostructured Silicas by Pseudomorphic Transformation: a Route towards Applications. *Adv. Funct. Mater.* **2006**, *16*, 1657-1667, DOI 10.1002/adfm.200500825.

(29) Yoo, W.C.; Stein, A. Solvent Effects on Morphologies of Mesoporous Silica Spheres Prepared by Pseudomorphic Transformations. *Chem. Mater.* **2011**, *23*, 1761-1767, DOI 10.1021/cm102829m.

(30) Bulut, A.; Yurderi, M.; Karatas, Y.; Say, Z.; Kivrak, H.; Kaya, M.; Gulcan, M.; Ozensoy, E.; Zahmakiran, M. MnOx-Promoted PdAg Alloy Nanoparticles for the Additive-Free Dehydrogenation of Formic Acid at Room Termperature. *ACS Catal.* **2015**, *5*, 6099-6110, DOI 10.1021/acscatal.5b01121.

(31) Song, F.-Z.; Zhu, Q.-L.; Tsumori, N.; Xu, Q. Diamine-Alkalized Reduced Graphene

Oxide: Immobilization of Sub-2 nm Palladium Nanoparticles and Optimization of Catalytic Activity for Dehydrogenation of Formic Acid. *ACS Catal.* **2015**, *5*, 5141-5144, DOI 10.1021/acscatal.5b01411.

(32) Bi, Q.-Y.; Lin, J.-D.; Liu, Y.-M.; He, H.-Y.; Huang, F.-Q.; Cao, Y. Dehydrogenation of Formic Acid at Room Temperature: Boosting Palladium Nanoparticle Efficiency by Coupling with Pyridinic-Nitrogen-Doped Carbon. *Angew. Chem. Int. Ed.* **2016**, *55*, 11849-11853, DOI 10.1002/anie.201605961.

(33) Wang, Z.-L.; Yan, J.-M.; Ping, Y.; Wang, H.-L.; Zheng, W.-T.; Jiang, Q. An Efficient CoAuPd/C Catalyst for Hydrogen Generation from Formic Acid at Room Temperature. *Angew. Chem. Int. Ed*. **2013**, *52*, 4406-4409, DOI 10.1002/anie.201301009.

(34) Wang, Z.-L.; Yan, J.-M.; Wang, H.-L.; Ping, Y.; Jiang, Q. Au@Pd Core-Shell Nanoclusters Growing on Nitrogen Doped Mildly Reduced Graphene Oxide with Enhanced Catalytic Performance for Hydrogen Generation from Formic Acid. *J. Mater. Chem. A.* **2013**, *1*, 12721-12725, DOI 10.1039/C3TA12531A.

TABLE OF CONTENTS (TOC) GRAPHIC

For Table of Contents Use Only.

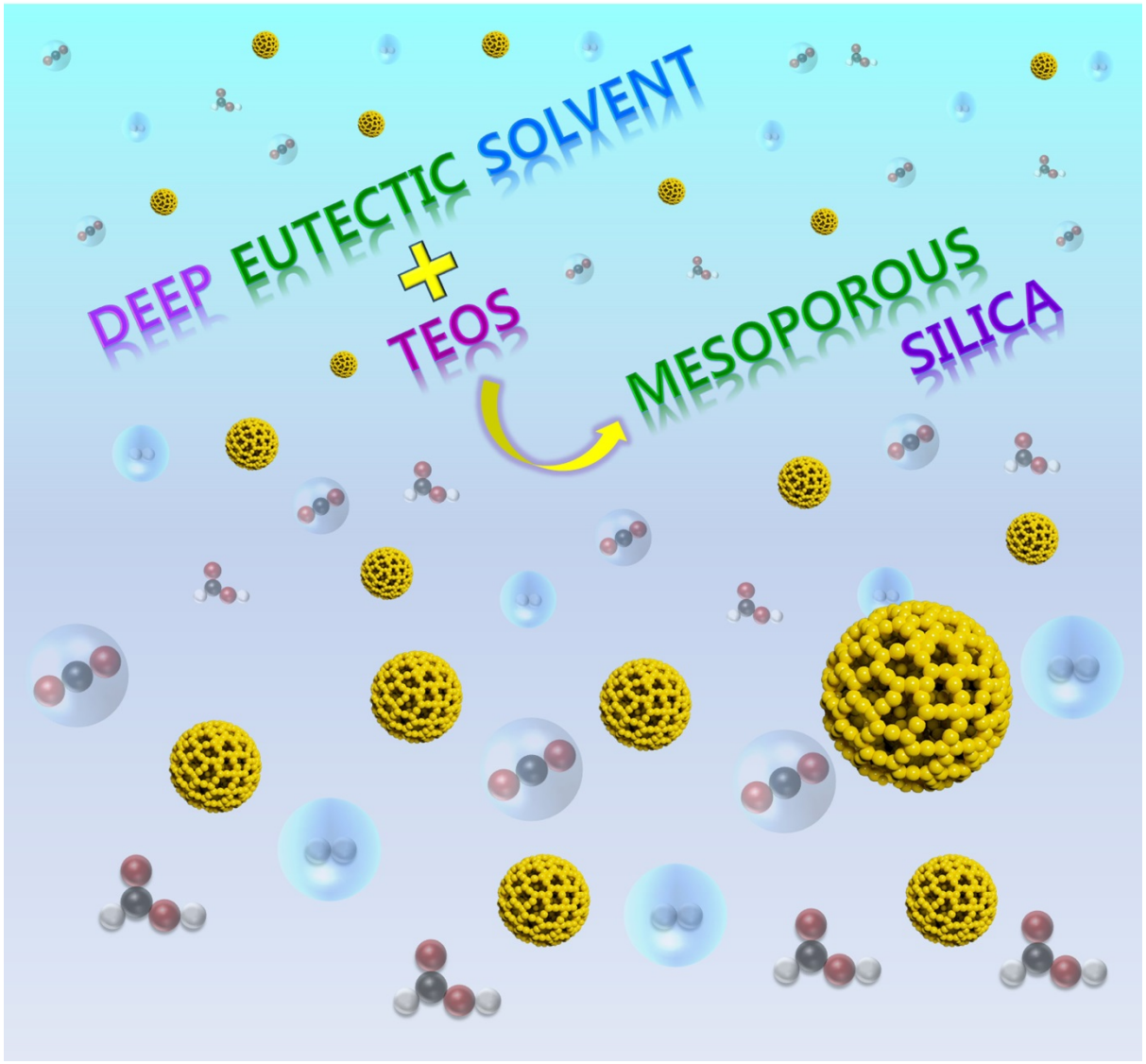

Table 1. Synthesis conditions of mesoporous silica materials.

Sample code	Addition amount of choline chloride/urea [g/g]	Addition amount of silica sol [mL]	Aging type	Aging temperature [^{o}C]
KIE-11-a	0/0	20	-	-
KIE-11-b	3.5/3	20	-	-
KIE-11-c	7/6	20	-	-
KIE-11-d	14/12	20	-	-
KIE-11-e	28/24	20	-	-
KIE-11-f	7/6	20	In a furnace	60
KIE-11-g	7/6	20	In a furnace	100
KIE-11-h	7/6	20	In a furnace	130
KIE-11-i	7/6	20	In a furnace	180
KIE-11-j	7/6	20	In an autoclave	100
KIE-11-k	7/6	20	In an autoclave	130
KIE-11-l	7/6	20	In an autoclave	180

Table 2. Pore properties of KIE-11 samples obtained from nitrogen sorption tests.

Sample code	SA_{BET} $[m^2/g]^a$	V_{tot} $[cm^3/g]^b$	D_{des} $[nm]^c$	D_{peak} $[nm]^d$
KIE-11-a	201	0.10	1.9	< 2.0
KIE-11-b	786	0.66	3.3	3.5
KIE-11-c	707	0.64	3.6	3.6
KIE-11-d	745	0.73	3.9	4.1
KIE-11-e	597	0.91	6.3	6.6
KIE-11-f	877	0.83	3.8	3.8
KIE-11-g	850	0.90	4.3	4.3
KIE-11-h	821	1.06	5.2	5.8
KIE-11-i	739	0.48	2.6	3.3
KIE-11-j	529	1.21	9.2	10.5
KIE-11-k	443	1.30	11.7	12.5
KIE-11-l	284	1.74	24.6	24.5

[a] BET surface area

[b] total pore volume taken from the volume of nitrogen adsorbed at P/Po=0.995

[c] desorption average pore diameter

[d] peak pore diameter

Figure Legend

Figure 1. (a) nitrogen sorption isotherms and (b) pore size distributions of KIE-11-a, KIE-11-b, KIE-11-c, KIE-11-d and KIE-11-e.

Figure 2. TEM image of mesoporous silica KIE-11-c (scale bar: 50 nm).

Figure 3. (a) nitrogen sorption isotherms and (b) pore size distributions of KIE-11-f, KIE-11-g, KIE-11-h, and KIE-11-i.

Figure 4. TEM images of (a) KIE-11-g and (b) KIE-11-i (scale bar: 50 nm).

Figure 5. TGA curves of (a) silica sol, (b) DES (choline chloride/urea), and (c) mixture of silica sol and DES (choline chloride/urea).

Figure 6. Schematic diagram of temperature range for condensation of silanol groups and for elimination of DES (choline chloride/urea), and suitable temperature range for aging in a muffle furnace.

Figure 7. (a) nitrogen sorption isotherms and (b) pore size distributions of KIE-11-j, KIE-11-k, and KIE-11-l.

Figure 8. TEM images of (a) KIE-11-j, (b) KIE-11-k, and (c) KIE-11-l (scale bar: 50 nm).

Figure 9. Schematic diagram for pore formation mechanism of KIE-11 prepared by using DES (choline chloride/urea) as a pore forming agent and solvent.

Figure 10. Formic acid dehydrogenation activity of Pd/NH_2-KIE-11-c, Pd/NH_2-KIE-11-k, and Pd/NH_2-KIE-11-l catalysts at room temperature.

Figure 11. STEM images of (a) Pd/NH_2-KIE-11-c, (b) Pd/NH_2-KIE-11-k, and (c) Pd/NH_2-KIE-11-l catalysts (scale bar: 20 nm). (Inset: Pd particle size distributions)

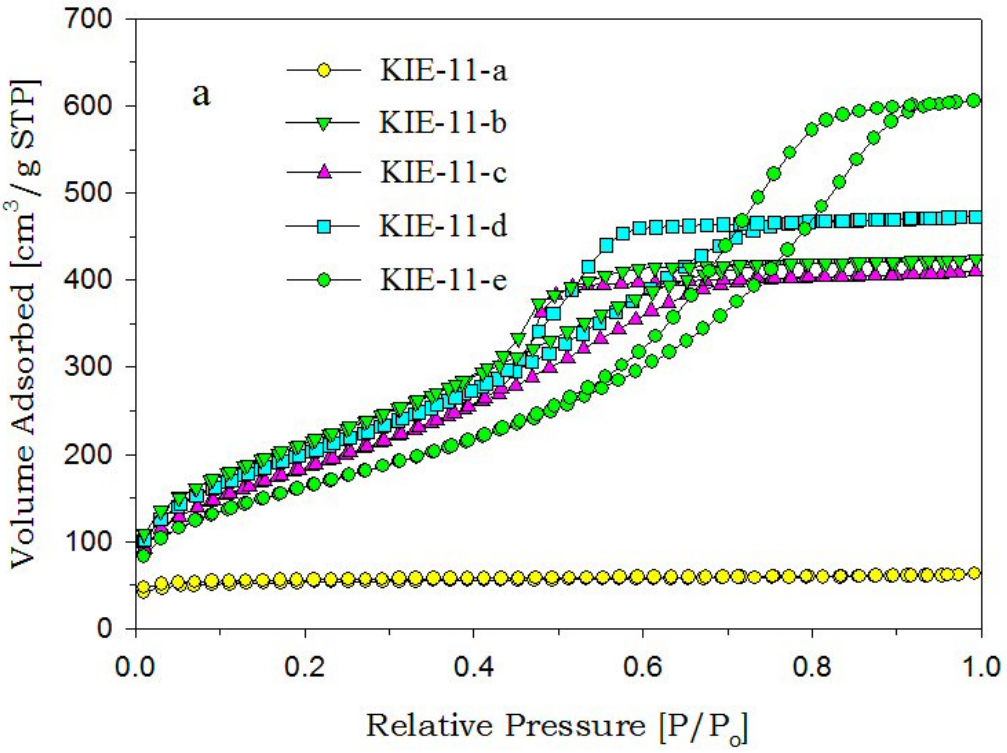
a
KIE-11-a
KIE-11-b
KIE-11-c
KIE-11-d
KIE-11-e
Volume Adsorbed [cm3/g STP]
Relative Pressure [P/Po]
0
100
200
300
400
500
600
700
0.0
0.2
0.4
0.6
0.8
1.0

Fig. 1a

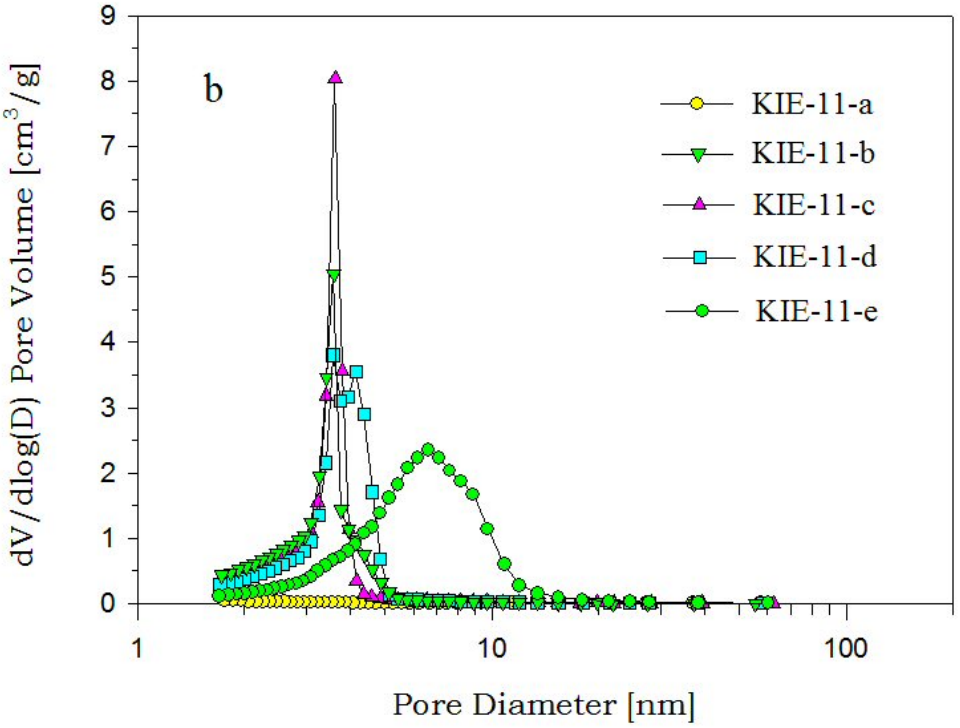
b
KIE-11-a
KIE-11-b
KIE-11-c
KIE-11-d
KIE-11-e
dV/dlog(D) Pore Volume [cm3/g]
Pore Diameter [nm]
0
1
2
3
4
5
6
7
8
9
1
10
100

Fig. 1b

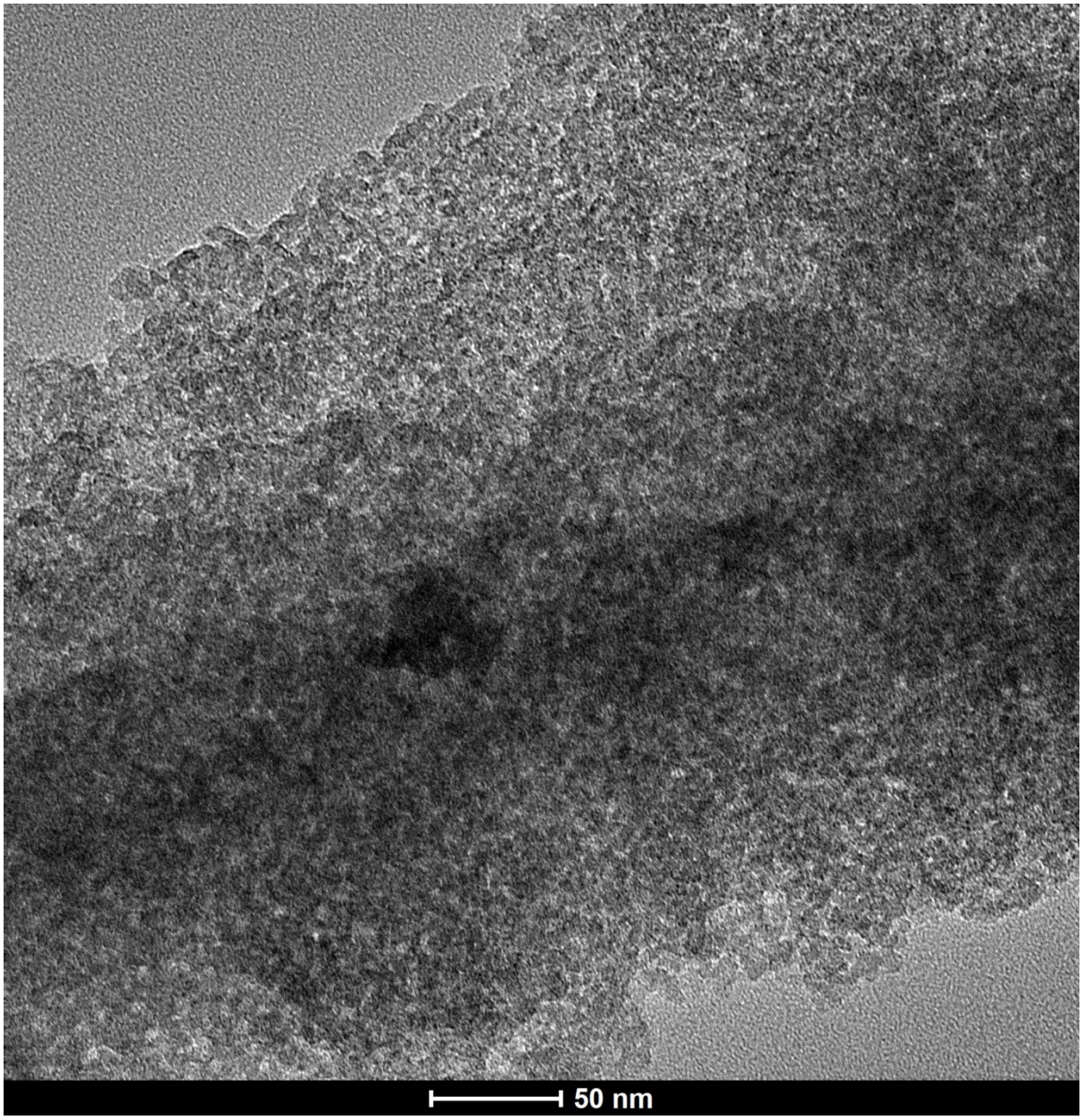

Fig. 2

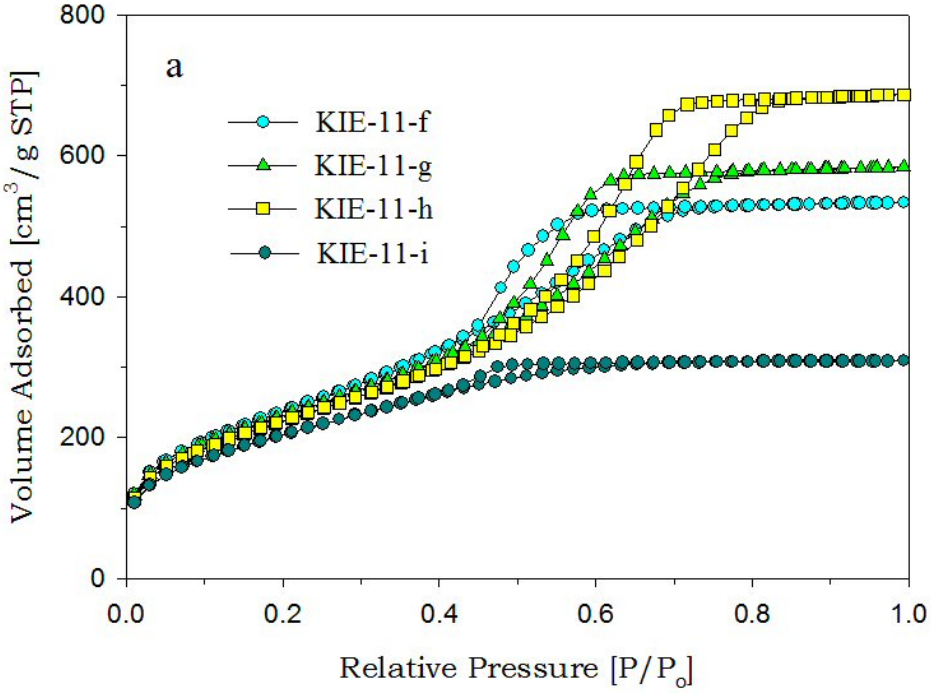
a
KIE-11-f
KIE-11-g
KIE-11-h
KIE-11-i
Volume Adsorbed [cm^3/g STP]
Relative Pressure [P/P$_o$]
0
200
400
600
800
0.0
0.2
0.4
0.6
0.8
1.0

Fig. 3a

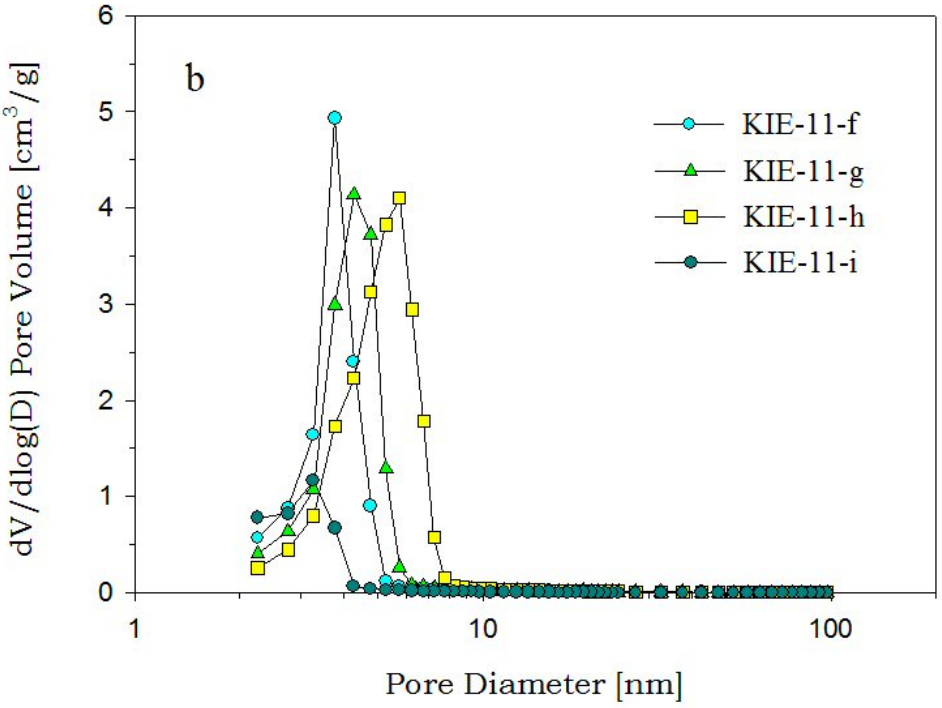
b
KIE-11-f
KIE-11-g
KIE-11-h
KIE-11-i
dV/dlog(D) Pore Volume [cm^3/g]
Pore Diameter [nm]
0
1
2
3
4
5
6
1
10
100

Fig. 3b

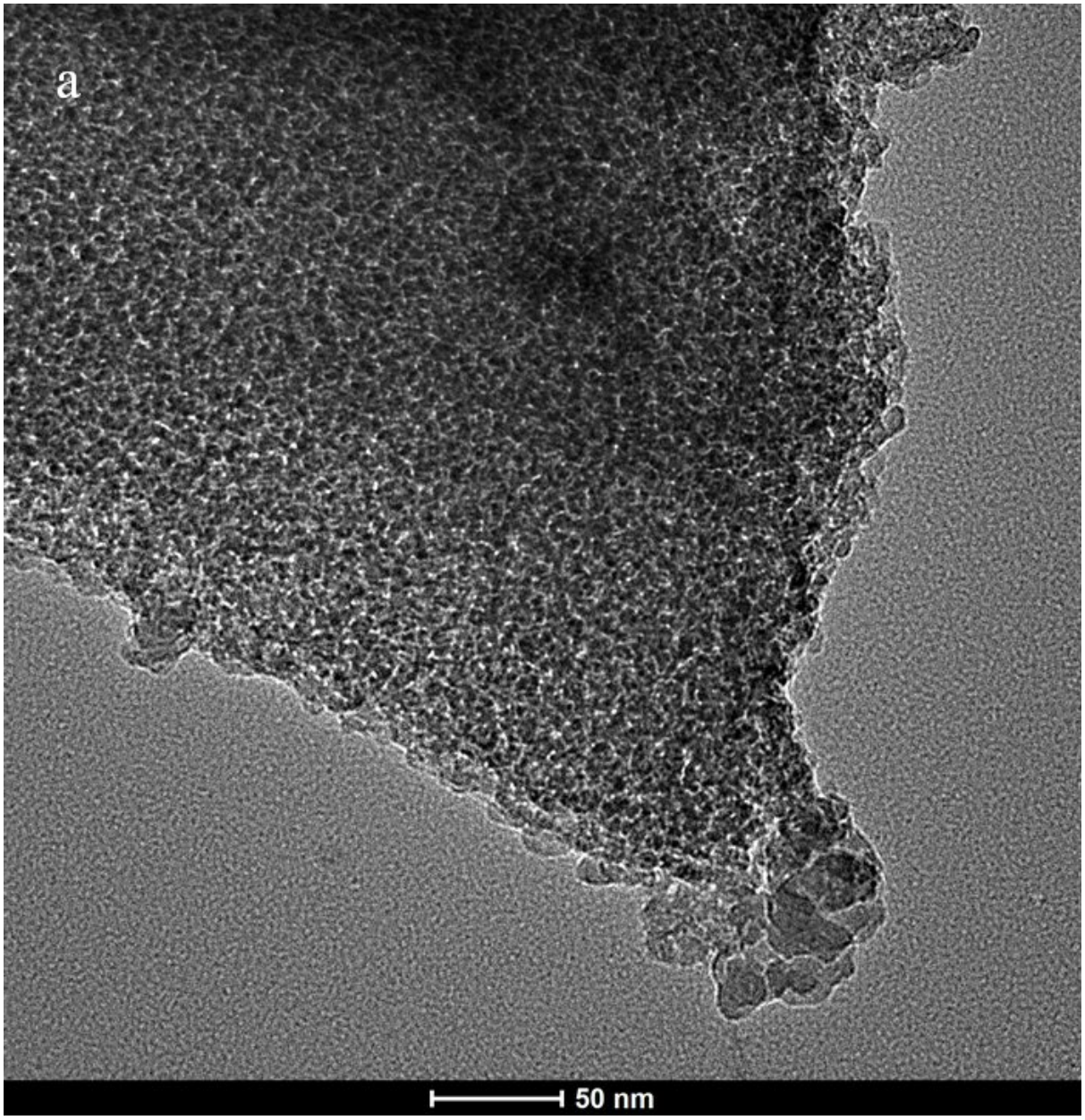

Fig. 4a

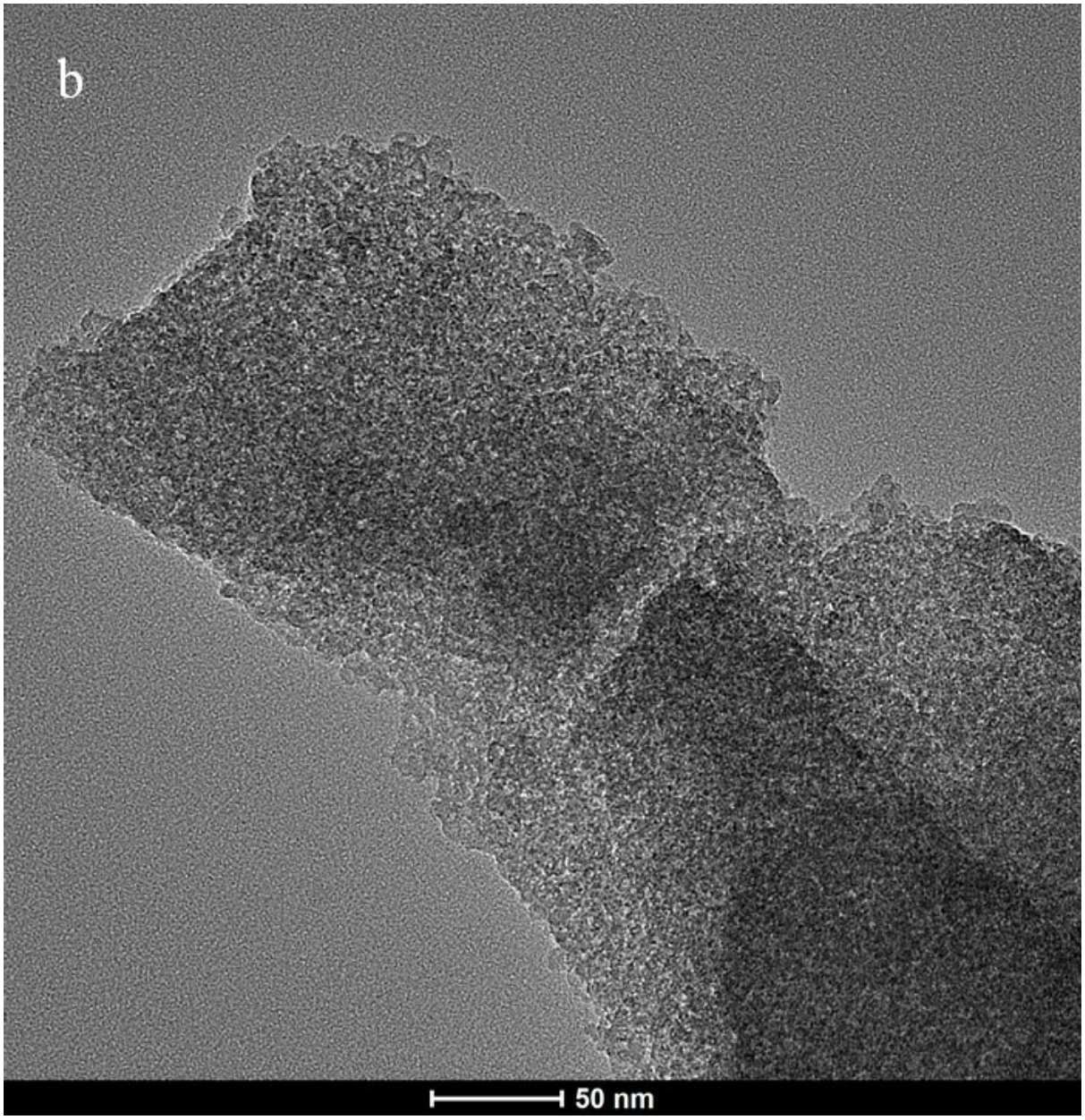

Fig. 4b

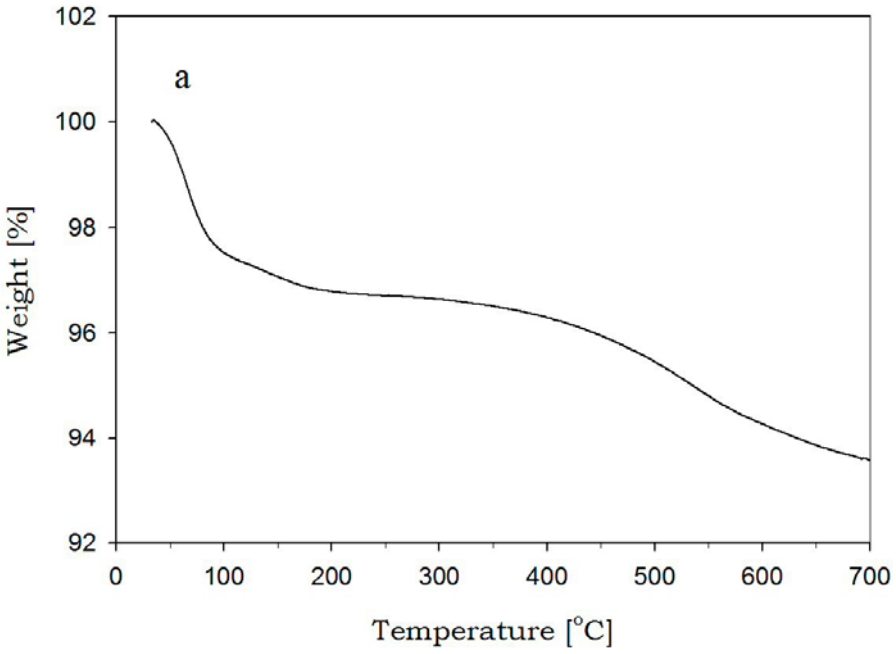
a
Weight [%]
Temperature [°C]
102
100
98
96
94
92
0
100
200
300
400
500
600
700

Fig. 5a

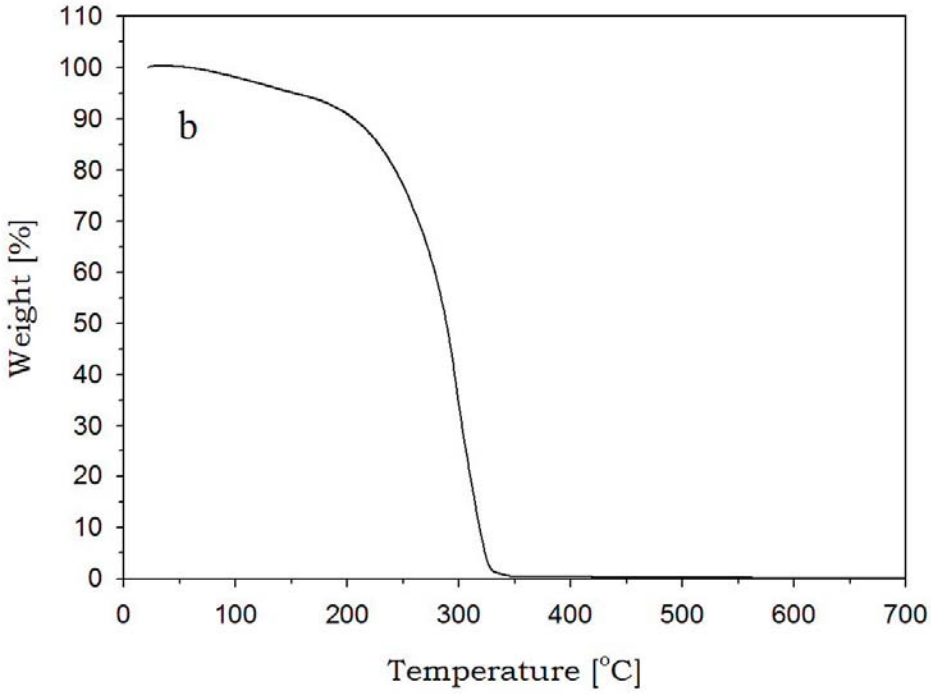
b
Weight [%]
Temperature [°C]
110
100
90
80
70
60
50
40
30
20
10
0
0
100
200
300
400
500
600
700

Fig. 5b

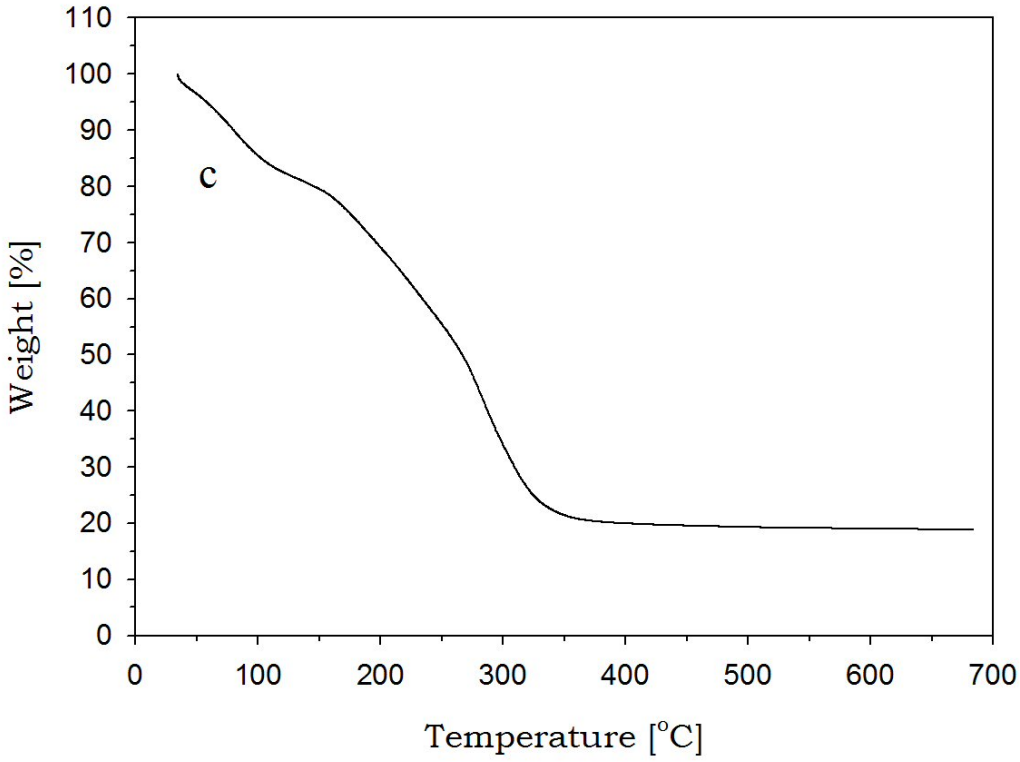
110
100
90
80
70
60
50
40
30
20
10
0
Weight [%]
C
0
100
200
300
400
500
600
700
Temperature [°C]

Fig. 5c

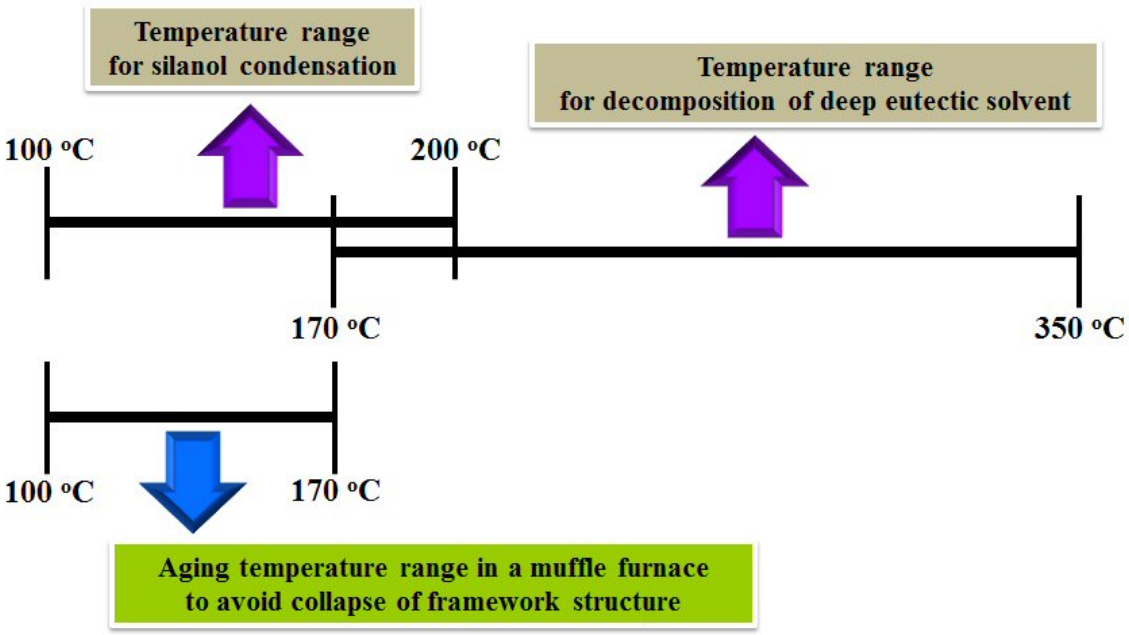
Temperature range
for silanol condensation
Temperature range
for decomposition of deep eutectic solvent
100 °C
200 °C
170 °C
350 °C
100 °C
170 °C
Aging temperature range in a muffle furnace
to avoid collapse of framework structure

Fig. 6

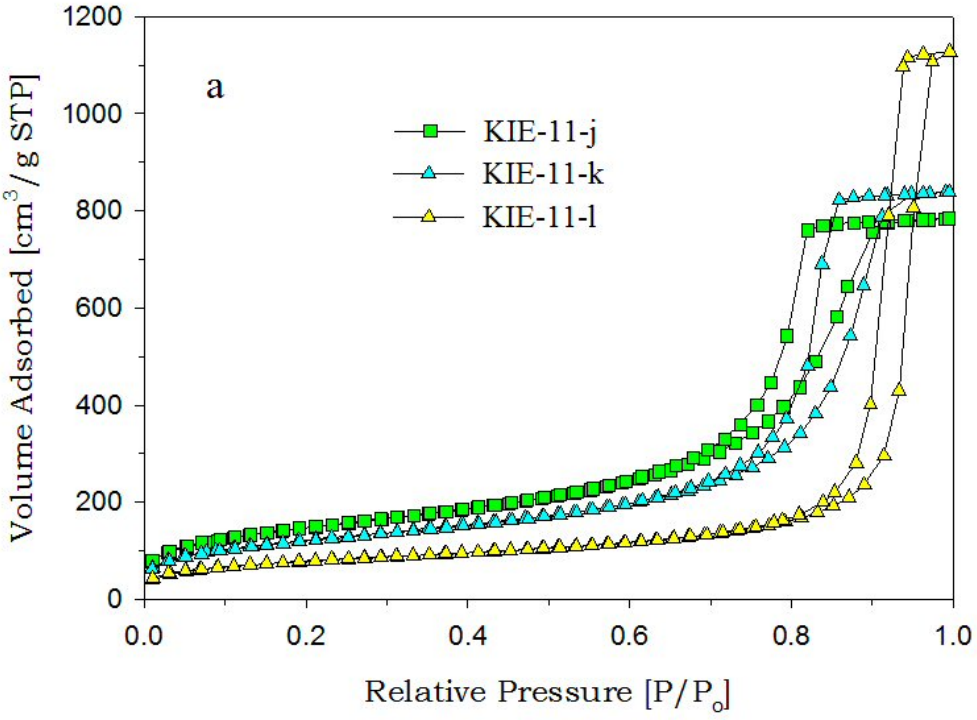
a
KIE-11-j
KIE-11-k
KIE-11-l
Volume Adsorbed [cm3/g STP]
Relative Pressure [P/Po]
0
200
400
600
800
1000
1200
0.0
0.2
0.4
0.6
0.8
1.0

Fig. 7a

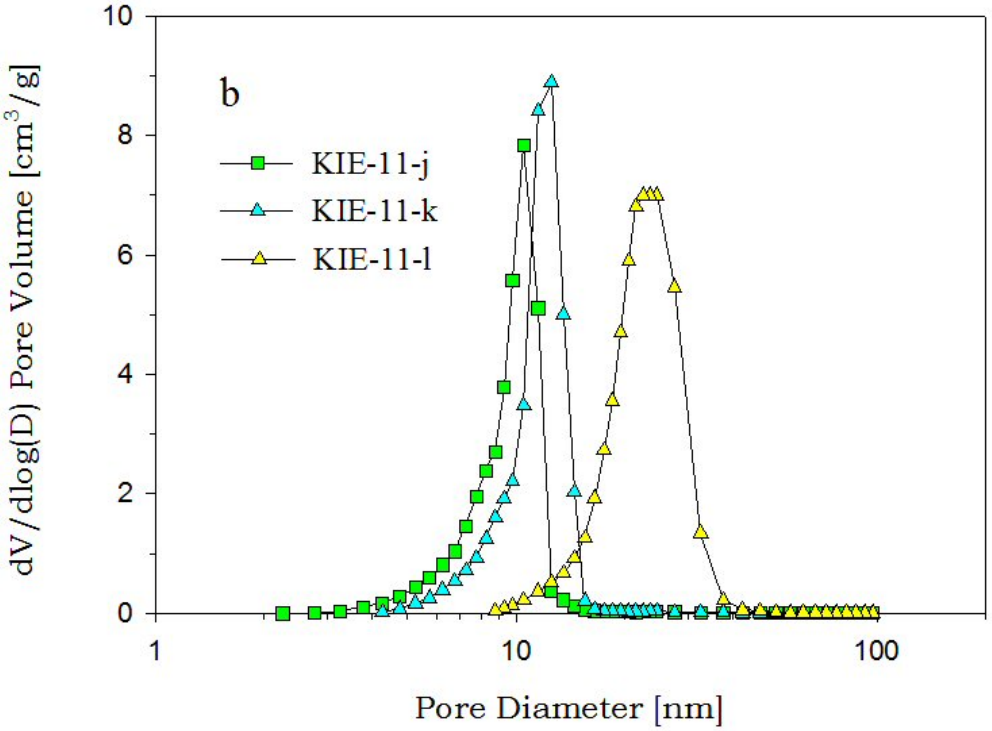
b
KIE-11-j
KIE-11-k
KIE-11-l
dV/dlog(D) Pore Volume [cm3/g]
Pore Diameter [nm]
0
2
4
6
8
10
1
10
100

Fig. 7b

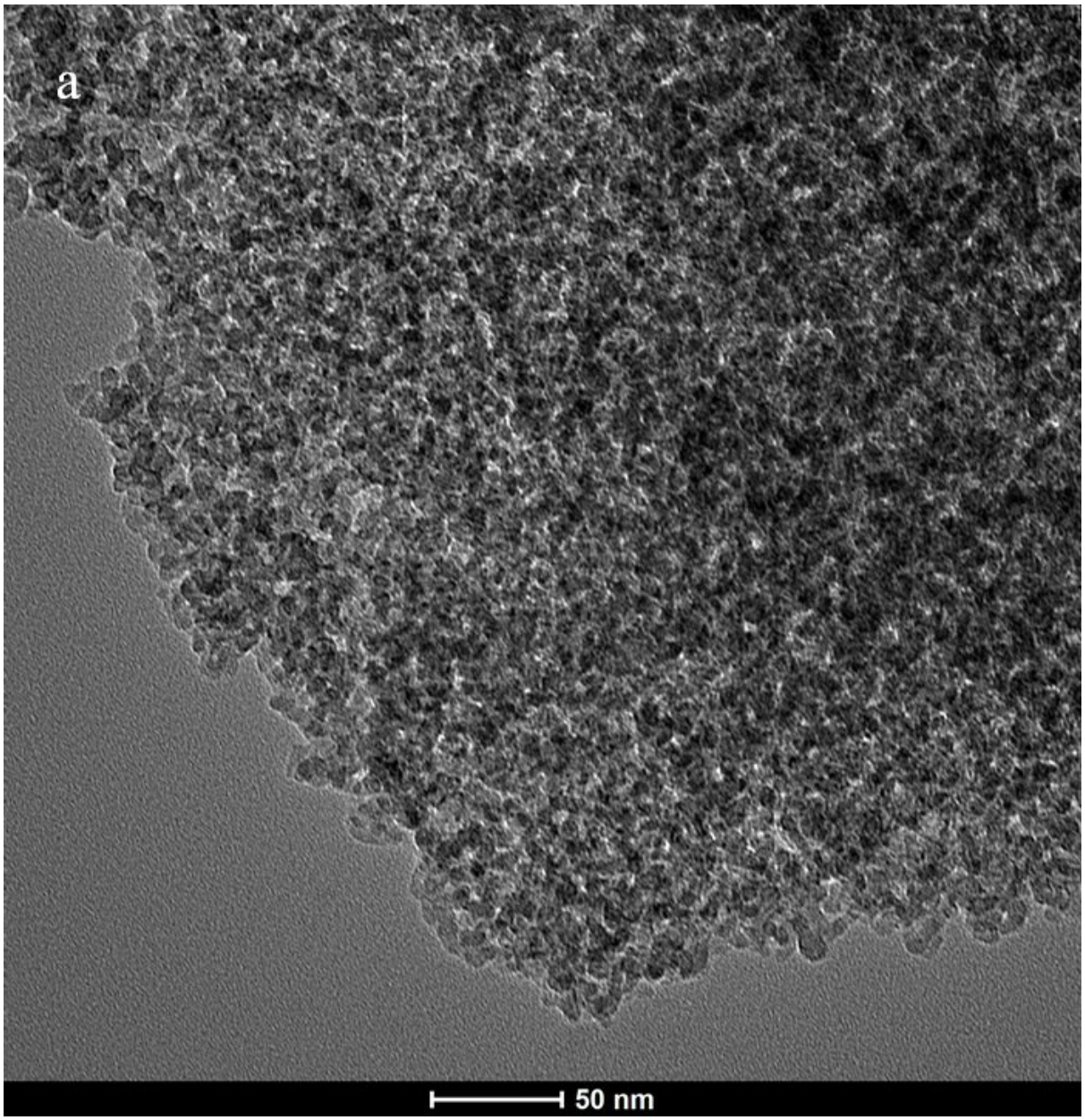

Fig. 8a

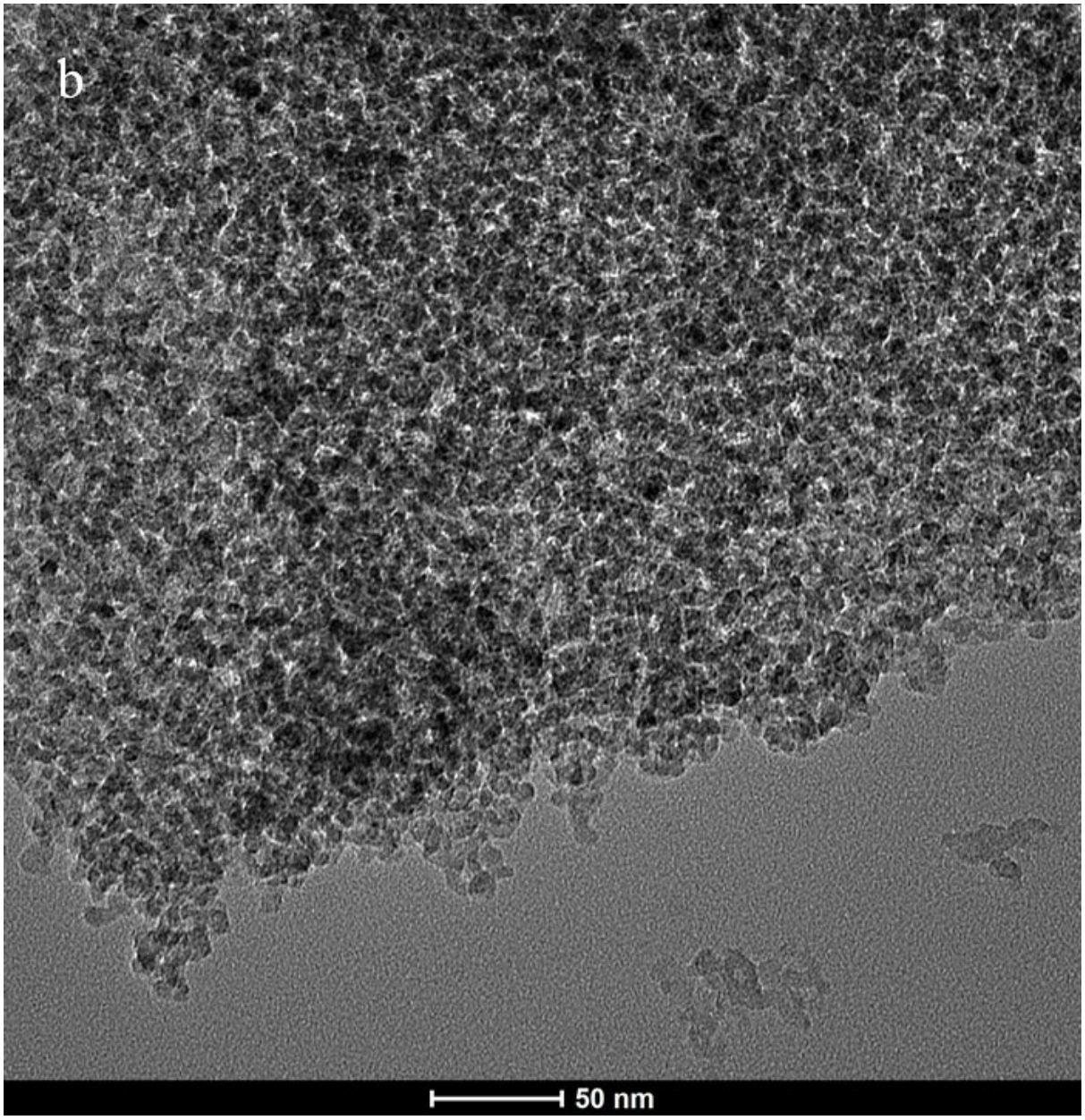

Fig. 8b

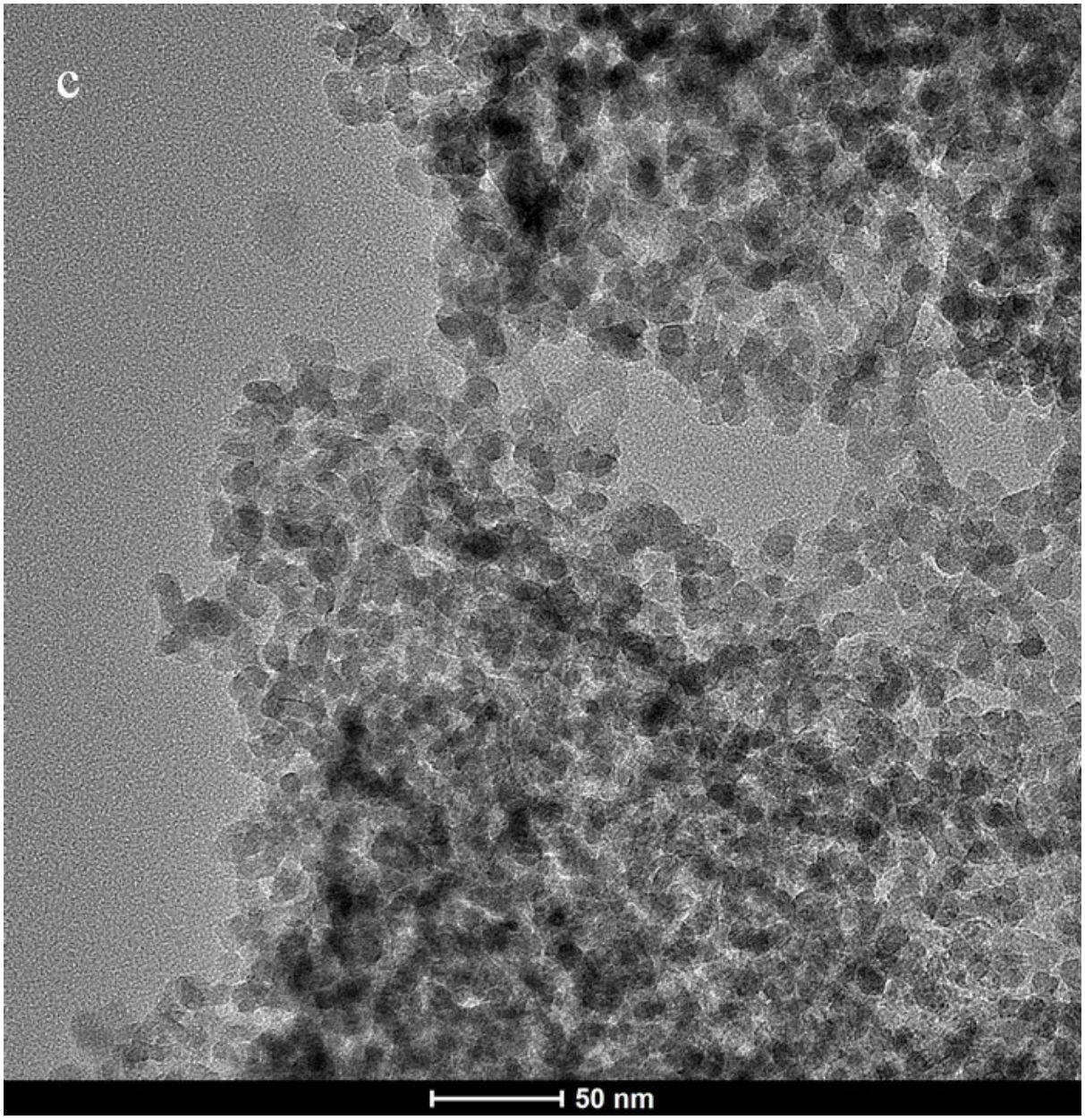

Fig. 8c

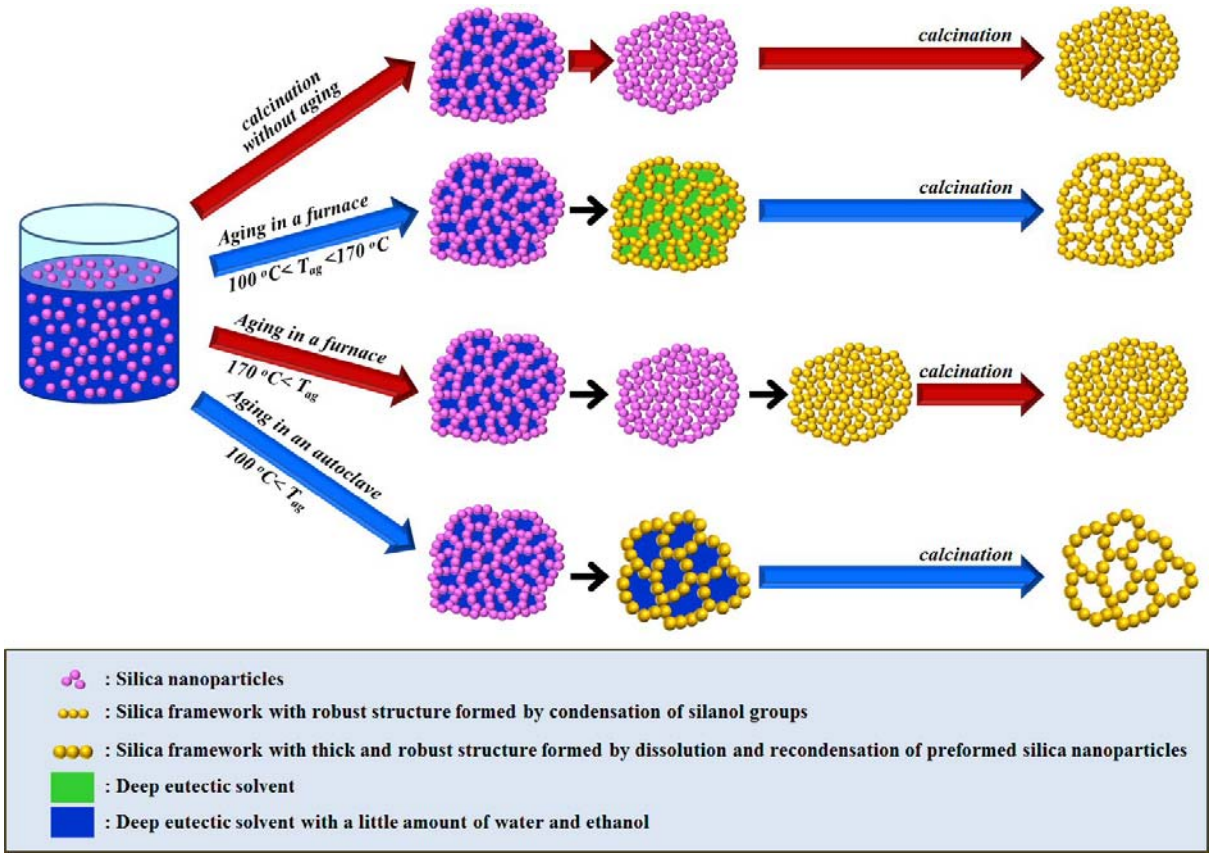
calcination without aging
Aging in a furnace
100 °C< T_ag <170 °C
Aging in a furnace
170 °C< T_ag
Aging in an autoclave
100 °C< T_ag
calcination
calcination
calcination
calcination
: Silica nanoparticles
: Silica framework with robust structure formed by condensation of silanol groups
: Silica framework with thick and robust structure formed by dissolution and recondensation of preformed silica nanoparticles
: Deep eutectic solvent
: Deep eutectic solvent with a little amount of water and ethanol

Fig. 9

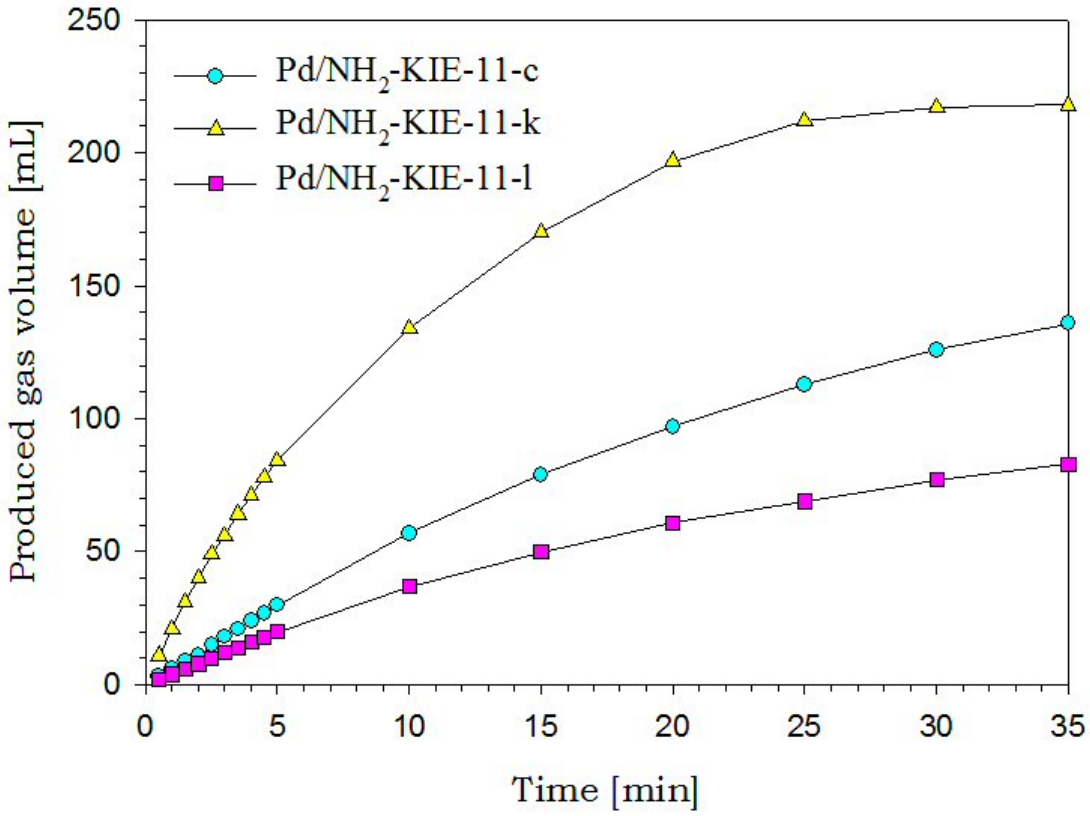
Pd/NH2-KIE-11-c
Pd/NH2-KIE-11-k
Pd/NH2-KIE-11-l
Produced gas volume [mL]
Time [min]
0
50
100
150
200
250
0
5
10
15
20
25
30
35

Fig. 10

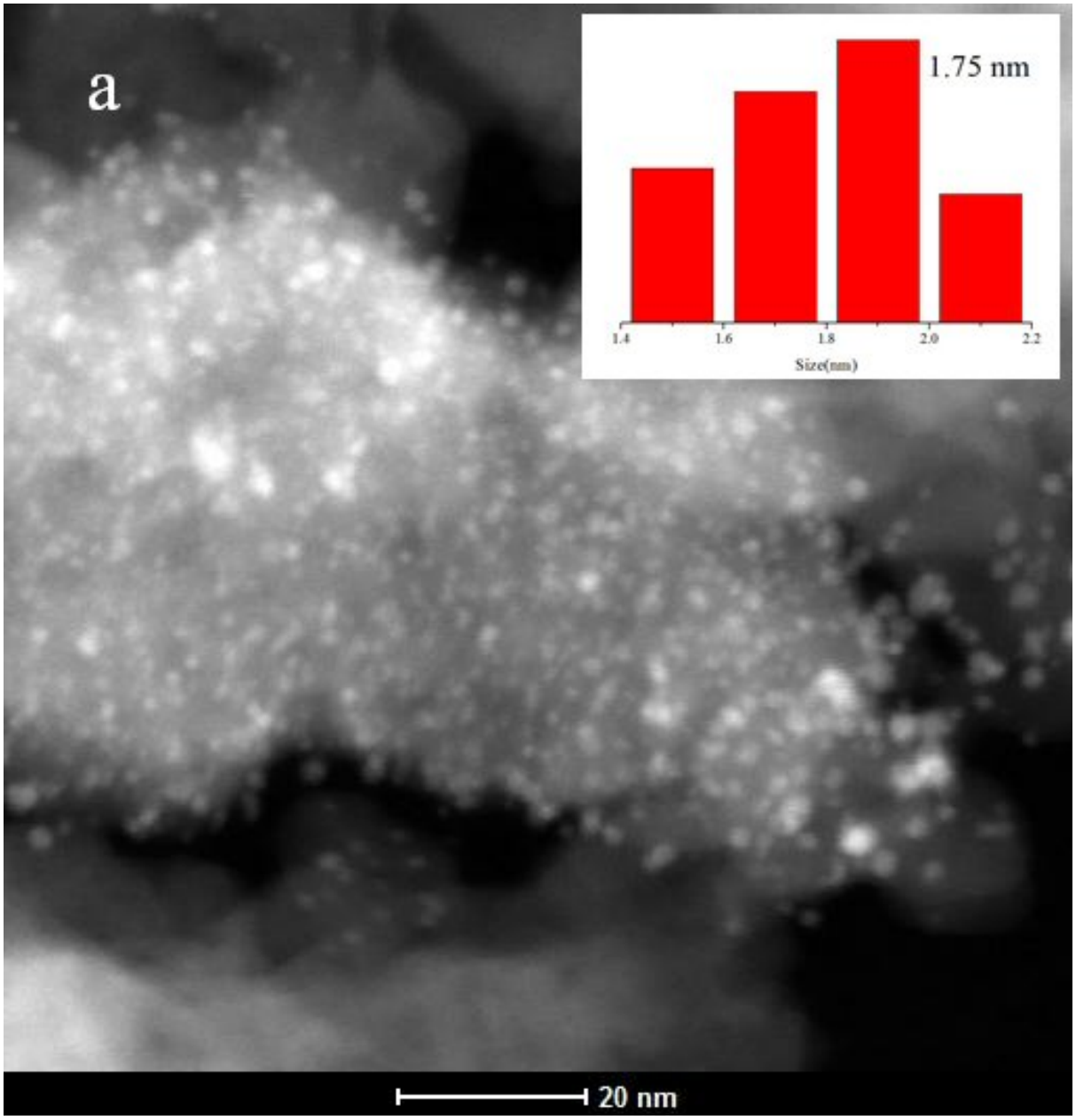

Fig. 11a

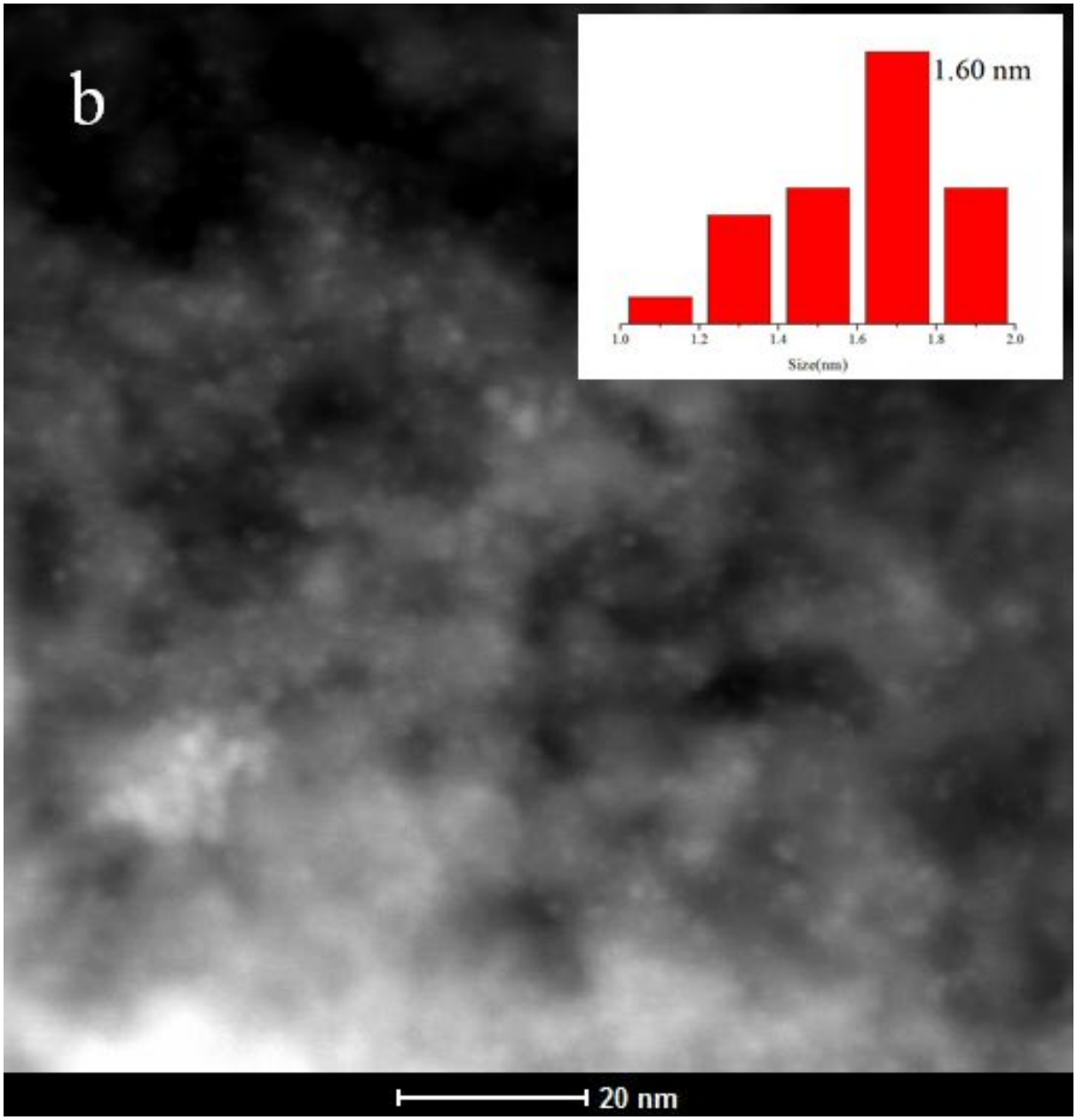

Fig. 11b

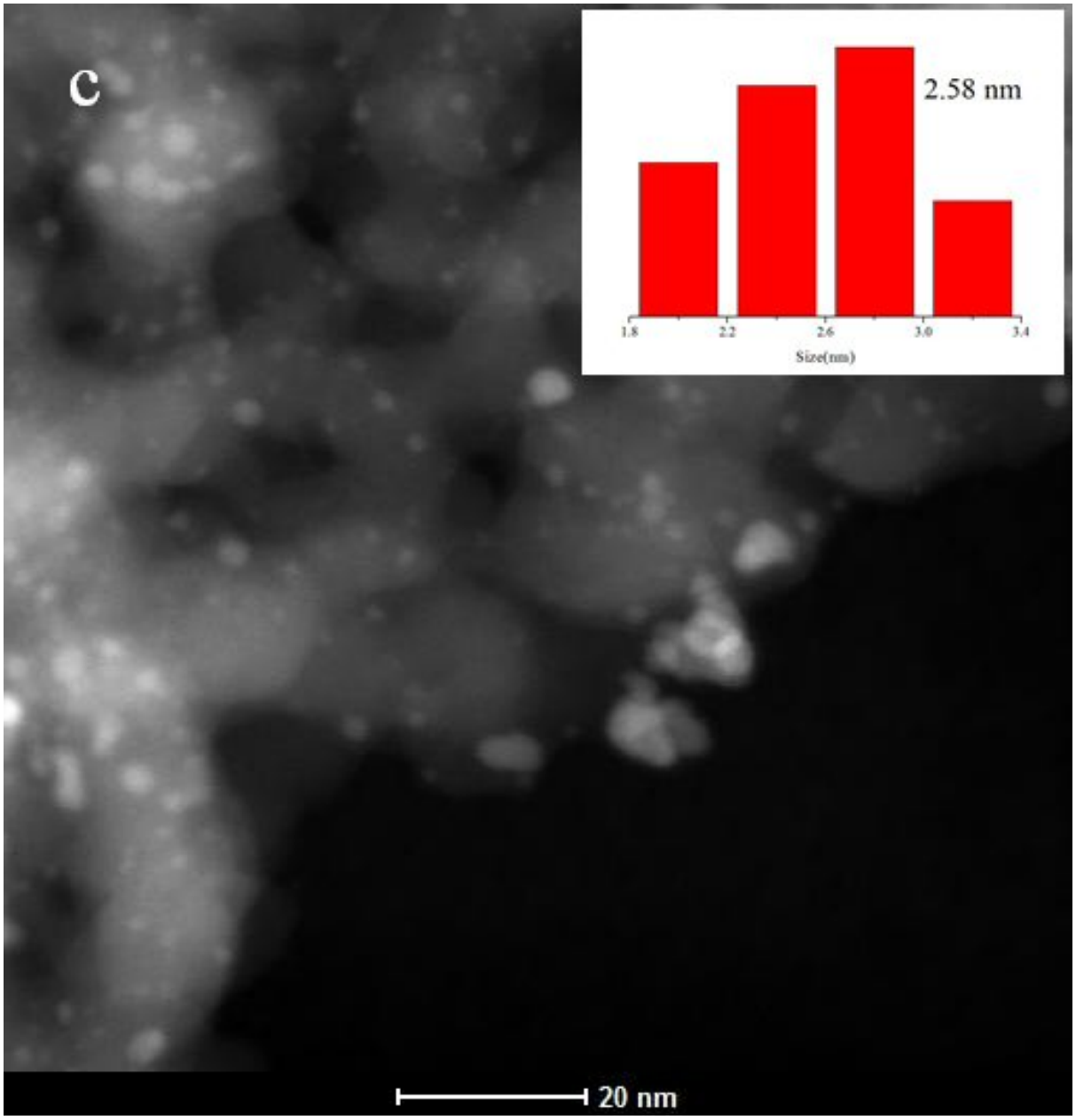

Fig. 11c

[**Graphic for manuscript**]

The development of more ecofriendly and economical synthetic pathways of mesoporous silica for its commercialization remains a challenge in the field of mesoporous silica synthesis. In this study, we first report a synthetic method of mesoporous silica (KIE-11) using deep eutectic solvent (DES) of choline chloride/urea as a templating agent and solvent without alcohol and water, except for water needed for hydrolysis of tetraethyl orthosilicate.